I&EC research
Industrial & Engineering Chemistry Research

Article

pubs.acs.org/IECR

Measurements and Modeling of Interfacial Tension for CO_2/CH_4/Brine Systems under Reservoir Conditions

Yueliang Liu,[†] Huazhou Andy Li,*[,†] and Ryosuke Okuno[‡]

[†]School of Mining and Petroleum Engineering, Faculty of Engineering, University of Alberta, Edmonton, Canada, T6G1H9
[‡]Petroleum & Geosystems Engineering, University of Texas at Austin, Austin, Texas 78712, United States

Supporting Information

ABSTRACT: Supercritical CO_2 injection is a promising way to hydraulically fracture tight/shale gas formations as well as enhance gas recovery from these formations. Understanding of phase behavior and interfacial tension (IFT) of CO_2/CH_4/brine (NaCl) systems is important, because they affect the performance of such a process in tight/shale gas formations. In this study, we employ the axisymmetric drop shape analysis (ADSA) method to measure the IFT between CO_2/CH_4 mixtures and brine over the temperature range from 77.0 to 257.0 °F and the pressure range from 15 to 5027 psia. Test results show that the presence of CO_2 decreases the IFT of CH_4/H_2O or CH_4/brine (NaCl) systems, while the degree of reduction depends on the molar fraction of CO_2 in the gas mixture. Salinity tends to cause an increase in IFT of CO_2/CH_4/brine (NaCl) systems; a higher salinity leads to an increased IFT for a given system. On the basis of the Parachor model (Weinaug and Katz *J. Ind. Eng. Chem.* **1943**, *35*, 239) and Firoozabadi's model (Firoozabadi and Ramey *J. Can. Pet. Technol.* **1988**, *27*, 41), we propose an improved IFT model to represent the measured IFT data for CO_2/CH_4/brine systems. The new IFT model preserves the principle of zero IFT at a critical point. Comparison of the new IFT model with four commonly used IFT correlations presented in the literature shows the superiority of the new model.

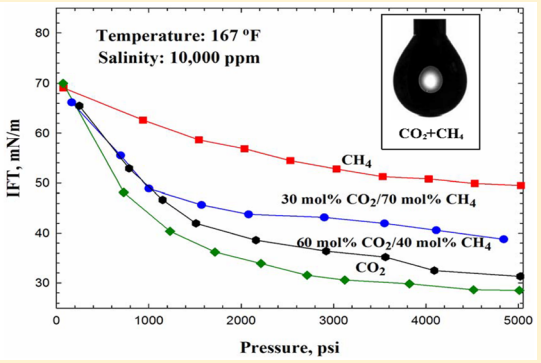

1. INTRODUCTION

Shale gas is playing an increasingly important role in the global energy portfolio since 2010; it accounted for 23% of total world energy supply in 2010 and will reach 49% in 2035, according to the report on annual outlook of global energy from USA energy information administration (EIA). Recent years have witnessed an increasing trend in developing new technologies for recovering the vast shale gas resources around the globe, such as hydraulic fracturing techniques. Waterless fracturing, such as CO_2 fracturing, has attracted extensive attention because of the unique properties of CO_2, such as a higher Langmuir adsorption in shale matrix compared to CH_4,[1] the compatibility between CO_2 and reservoir fluids (CH_4 and water), and large diffusivity of CO_2 in shale pores. These properties might enable CO_2-based fracturing technique to mitigate the formation damage issues that are otherwise caused by water-based fracturing, hence promoting a higher gas recovery post fracturing. Enhancing shale gas recovery through injecting CO_2 is also under investigation in some shale reservoirs.[2] Additional benefits of using CO_2 include storing CO_2 in shale formations. Either CO_2-based fracturing or CO_2-based enhanced gas recovery requires a profound understanding on the phase behavior and interfacial properties of the CO_2/CH_4/brine systems under reservoir conditions.[3]

Interfacial tension (IFT) of gas−water or gas−brine is one of the most important properties affecting the performance of enhanced gas recovery. It significantly affects the movement, phase behavior, and distribution of reservoir fluids in porous media.[4] Specifically, optimum operations of CO_2 flooding and sequestration in oil/gas reservoirs also depend on accurate knowledge of IFT of CO_2/brine systems, which affect the transport properties and capillary-sealing efficiency of CO_2 in the formation.[5−8]

There have been extensive experimental and modeling studies on quantifying the IFT of various gas−water systems. Axisymmetric drop shape analysis method (ADSA) is the most-widely used technique to perform IFT measurement. With the ADSA method, IFT is measured by solving the Young−Laplace equation based on the geometry of a pendant drop captured by the measurement.[9,10] Table 1 summarizes some of the relevant gas−water IFT measurements and the range of laboratory conditions under which the measurements were conducted. It can be seen from Table 1 that extensive experimental studies have been conducted on pure gas−pure water systems over wide ranges of pressures and temperatures. Most of the existing studies did not address the effects of nonhydrocarbon contaminants on gas−water IFT, especially at high pressure/

Received: June 26, 2016
Revised: November 9, 2016
Accepted: November 9, 2016
Published: November 10, 2016

DOI: 10.1021/acs.iecr.6b02446
Ind. Eng. Chem. Res. 2016, 55, 12358−12375

Table 1. Summary of Previous Laboratory Measurements on Gas−Water IFT

references	system compositions	temperature range, °F	pressure range, psia
Hocott[57] 1939	$CH_4/C_2H_6/C_3H_8/H_2O$	78.0−150.0	14.5−3,510
Hough et al.[53] 1951	CH_4/H_2O	74.0−280.0	15−15 000
Heuer[58] 1957	CO_2/H_2O	100.0, 280.0	up to 10 000
Jennings and Newman[54] 1971	CH_4/H_2O	74.0, 212.0, 350.0	14.7−12 000
Massoudi and King[27] 1974	CH_4/H_2O, CO_2/H_2O, N_2/H_2O	77.0	up to 1000
Jho et al.[78] 1978	CO_2/H_2O	32.0−122.0	60−1000
Wiegand and Franck[72] 1994	$CH_4/C_3H_8/C_6H_{14}/C_{10}H_{22}/N_2/H_2O$, etc.	77.0−571.0	14.5−37,710
Chun and Wilkinson[59] 1995	CO_2/H_2O/ethanol	41.0−160.0	14.5−2700
Sachs and Meyn[55] 1995	CH_4/H_2O	77.0	58−6802
Lepski[79] 1997	CH_4/H_2O, N_2/H_2O	126.5−260.2	1500−3500
Tian et al.[80] 1997	CH_4/H_2O, C_6H_{14}/H_2O, C_7H_{16}/H_2O, N_2/H_2O, etc.	76.7−400.0	14.7−29 008
da Rocha et al.[60] 1999	CO_2/H_2O	95.0−149.0	1000−4000
Ren et al.[11] 2000	CH_4/H_2O, $CH_4/CO_2/H_2O$	77.0−212.0	145−4351
Yan et al.[34] 2001	$CH_4/N_2/H_2O$, $CO_2/N_2/H_2O$	77.0−212.0	145−4351
Hebach et al.[31] 2002	CO_2/H_2O	41.0−144.0	14.5−2900
Zhao et al.[81] 2002	CH_4/H_2O	77.0−212.0	145−4351
Tewes and Bourey[82] 2005	CO_2/H_2O	68.0, 86.0, 104.0	290−1305
Park et al.[61] 2005	CO_2/H_2O	68.0, 77.0, 100.4, 159.8	up to 2941
Yang et al.[20] 2005	CO_2/brine	77.0, 136.0	14.5−4351
Chiquet et al.[62] 2007	CO_2/H_2O	95.0−230.0	725−6527
Akutsu et al.[83] 2007	CO_2/H_2O	77.0, 95.0, 113.0	1088−2393
Sutjiadi-Sia et al.[84] 2008	CO_2/H_2O	104.0	up to 3916
Bennion and Bachu[21] 2008	CO_2/H_2O/brine	105.0−257.0	290−3916
Rushing et al.[76] 2008	$CH_4/C_2H_6/C_3H_8/N_2/CO_2/H_2O$	300.0−400.0	1000−20 000
Bachu and Bennion[23] 2009	CO_2/H_2O/brine	68.0−257.0	290−3916
Aggelopoulos et al.[7] 2010	CO_2/brine	81.0−212.0	725−3626
Georgiadis et al.[63] 2010	CO_2/H_2O	77.0−214.0	145−4351
Chalbaud et al.[22] 2010	CO_2/brine	81.0−212.0	3771
Shariat et al.[85] 2011	$CH_4/C_2H_6/C_3H_8/H_2O$	300.0−400.0	1000−20 000
Aggelopoulos et al.[86] 2011	CO_2/brine	80.6, 159.8, 212.0	725−3626
Shariat et al.[87] 2012	CO_2/H_2O	up to 400.0	1000−18 000
Li et al.[13] 2012	CO_2/brine	76.7−346.7	290−7252
Li et al.[14] 2012	CO_2/brine	157.7−301.7	290−7252
Khosharay and Varaminian[56] 2014	CH_4/H_2O, C_2H_6/H_2O, CO_2/H_2O, C_3H_8/H_2O	51.8−102.2	up to 870
Pereira et al.[88] 2015	CO_2/H_2O	76.7−384.5	49−10 028
Khashefi et al.[15] 2016	CH_4/H_2O, CH_4/brine	100.1−391.7	0−13 343

temperature reservoir conditions. Moreover, most of the gas/water IFT measurements are only made for the pure hydrocarbon gases, rather than gas mixtures, with water or brine. Ren et al.[11] measured the interfacial tension of $CH_4/CO_2/H_2O$ systems. They covered the temperature range of 76.7−211.7 °F and pressure range of 145−4351 psia. But the salinity effect on the IFT was not addressed.

In shale formations, the presence of salinity can affect the IFT of reservoir fluids to a large extent. It has been recognized that the addition of salts into the aqueous phase can significantly increase the IFT of gas/brine systems.[12−14] Some of the previous studies attributed the salinity effect to the change of the interface structure: the cations tend to accumulate in the aqueous phase due to the adsorption of the cations on the interface.[15−19] Another reason causing the IFT increase is the density increase of the aqueous phase because of salt addition. Yang et al.[20] reported IFT for CO_2/brine system over 77.0−136.0 °F and 14.5−4351 psia. Bennion and Bachu[21] measured the IFT for CO_2/brine system over 105.0−257.0 °F and 290−3916 psia. Aggelopoulos et al.[7] presented the IFT data of CO_2/brine system, with the consideration of different concentrations of NaCl and $CaCl_2$. Chalbaud et al.[22] measured the IFT for CO_2/brine systems at salinities of 0.085−2.75 mol/kg. Khashefi et al.[15] carried out IFT measurements on CH_4/brine and CH_4/pure water systems using the ADSA method in the temperature range 100.1−391.7 °F and at pressures up to 13343 psia. Bachu and Bennion[23] conducted the IFT measurement of CO_2/water and CO_2/brine systems over 68.0−257.0 °F and 290−3916 psia. Li et al.[13,14] measured the IFT between CO_2 with different salts in a wide range of total salt molality. Nonetheless, the experimental data for IFT of CH_4/brine mixtures are limited. Meanwhile, experimental data for IFT of CO_2/CH_4/brine mixtures are still scarce at reservoir conditions, albeit extensive IFT measurements have been conducted for CO_2/brine mixtures in the past decades.

An accurate IFT model is needed to predict the IFT of gas/brine systems under reservoir conditions. Up to now, numerous correlations were proposed and some of them have been used in commercial reservoir simulators for estimating IFT by petroleum engineering industry. The Parachor model[24,25] and the scaling law[26] have gained more use than other predictive methods because of their simplicity.[4] However, both methods are not recommended for IFT predictions of hydrocarbon/water systems.[4] Massoudi and King[27] presented an IFT correlation for pure CO_2/water systems considering pressure

DOI: 10.1021/acs.iecr.6b02446
Ind. Eng. Chem. Res. 2016, 55, 12358−12375

and temperature; but it can be only applied at one temperature. Firoozabadi and Ramey[28] proposed an IFT model that can predict the IFT of hydrocarbon-gas/water mixtures. Argaud[29] and Sutton[30] developed new IFT correlations based on the Firoozabadi and Ramey[28] model by considering a broader class of compounds. Argaud[29] added the ratio of Parachor to molar mass of each compound to the Firoozabadi and Ramey[28] correlation as a corrective factor, while Sutton[30] considered more parameters in the improved correlation. Nonetheless, the predictive capabilities of these improved models are still limited.[17] Bennion and Bachu[21] presented an IFT correlation between CO_2 and brine as a function of salinity, which predicts the IFT of CO_2/brine systems based on the solubility of CO_2 in brine. However, the correlation of Bennion and Bachu[21] cannot predict IFT at pressures and temperatures higher than 3916 psia and 257.0 °F. Meanwhile, the correlation was developed based on their own measured data, without being validated by other experimental data. Hebach et al.[31] and Kvamme et al.[32] presented IFT correlations for CO_2/water mixtures considering reservoir temperature, pressure, and density differences of pure component, but excluding the effect of mutual solubility. Furthermore, Li et al.[13,14] and Chalbaud et al.[33] developed correlations for IFT of CO_2/brine mixtures. Other methods based on statistical thermodynamics were also applied to predict IFT, such as linear gradient theory,[34] perturbation theory,[35] density gradient theory (DGT),[36,37] and integral and density functional theories.[38−40] In general, these methods have not been widely used in the petroleum industry likely due to their complexity.

In this study, previous IFT measurements of the gas/water or gas/brine mixtures are first reviewed and summarized. New experimental IFT data for CO_2/CH_4/brine systems with NaCl concentrations up to 200 000 ppm are presented over 77.0−257.0 °F and 15−5027 psia. IFT data for CH_4/water and CO_2/water mixtures are found to be in good agreement with published data. The effects of temperature, pressure, CO_2 concentration, and salinity on IFT of CO_2/CH_4/brine mixtures are examined in detail. Based on the measured IFT data, a new IFT model is developed to determine IFT of CO_2/CH_4/brine mixtures. We examine this new model's performance by comparing it with other commonly used IFT correlations.

2. EXPERIMENTAL SECTION

2.1. Materials. Distilled water was used in the experiment. CO_2 and CH_4 (Praxair, Canada) have purities of 99.998 mol % and 99.99 wt %, respectively. Sodium chloride, ACS grade with a purity of greater than 99 wt %, was supplied by Sigma-Aldrich Company (Canada).

2.2. Experimental Setup. Figure 1 shows an image of the experimental setup used for the ADSA IFT measurements. The major component of this system is a visual high-pressure cell (TEMCO, Inc., U.S.A.) with a chamber volume of approximately 41.5 cm^3. It can sustain pressure up to 10130.9 psia and temperature up to 350.0 °F. A light source was used to illuminate the pendant drop in the glass-windowed chamber. Nitrile O-rings were used in this experiment to reduce the corrosion of O-rings caused by CO_2 exposure. A band heater, together with an insulation jacket and a resistance temperature device (RTD) sensor, was used to heat the IFT cell and control its temperature within ±0.1 K. The IFT cell was placed on a vibration-free table (RS4000, USA) to remove the effect of constant low-frequency vibration. A needle valve was employed for controlling the formation of pendant drop, while several

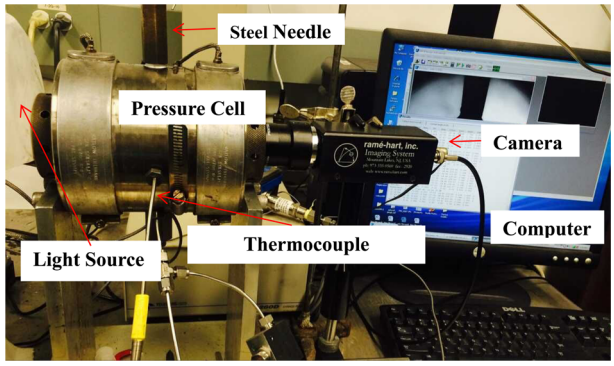

Figure 1. Digital image of the ADSA experimental setup.

other valves were used to control the introduction of the different fluids (e.g., CO_2 or CH_4) into the pressure cell. The drain valve and a needle cleanout valve were used to flush and clean the cell chamber and needle without removal of the glass windows. A high-resolution camera was used to observe the formation of the pendant drop, and capture its image. The stainless-steel needles could be changed to cover different IFT measurement ranges.

Figure 2 shows the schematic of the ADSA experimental setup used in this study. The pressure of the high pressure IFT cell was measured with a digital precision testing gauge (DPG409-5.0kG, Ashcroft) with an accuracy of 0.05% of the full range. The temperature was measured with a thermocouple (JMQSS-125U-6, Omega) with an accuracy of ±0.1 K. The LED light source with a glass diffuser was used to provide a uniform illumination for the pendant drop. Two transfer cylinders, connected to the IFT cell, were used to pressurize and inject CH_4 and CO_2. The pressure of transfer cylinders was controlled by a syringe pump (500 HP, ISCO, Inc., Lincoln, NE). In this study, the pressure measurement, temperature measurement, and determination of mixture composition have accuracies of ±3 psia, ± 0.1 K, and ±3.0 wt %, respectively. Considering the inaccuracies that arise from the ASDA method as well as from the estimated phase densities, a conservative uncertainty of ±5% can be applied to the experimentally measured IFTs. The IFT of the CO_2/CH_4/brine systems is measured over 77.0−257.0 °F, 15−5,027 psia, and a salinity range of 0−200 000 ppm of NaCl. Each IFT measurement was repeated three times to ensure the repeatability of each measurement.

2.3. Experimental Procedures. Before each measurement, the entire system was tested for leakage with N_2. Then it was cleaned with acetone, flushed with CH_4 or CO_2 and evacuated. The cell was pressurized with CH_4 or CO_2 to a prespecified pressure. When measuring the IFT for gas mixtures, the pressure cell was first filled with a pure gas (e.g., CO_2) to a specified pressure at a given temperature; then another pure gas (e.g., CH_4) was injected into the pressure cell, resulting in a different pressure. A sampler (Swagelok, Canada) with a volume of 10 cm^3 was used to take the gas sample inside the pressure cell. The composition of the gas mixture was measured with a gas chromatography (GC) method. After the pressure and temperature in the pressure cell were stabilized, a pendant water/brine drop was introduced by a syringe pump (500 HP, ISCO, Inc., Lincoln, NE), of which pressure was maintained about 14−44 psia higher than that of gas phase inside the pressure cell. The pendant water drop formed at the tip of the stainless-steel needle. After the gas was injected, usually 30−60

DOI: 10.1021/acs.iecr.6b02446
Ind. Eng. Chem. Res. 2016, 55, 12358−12375

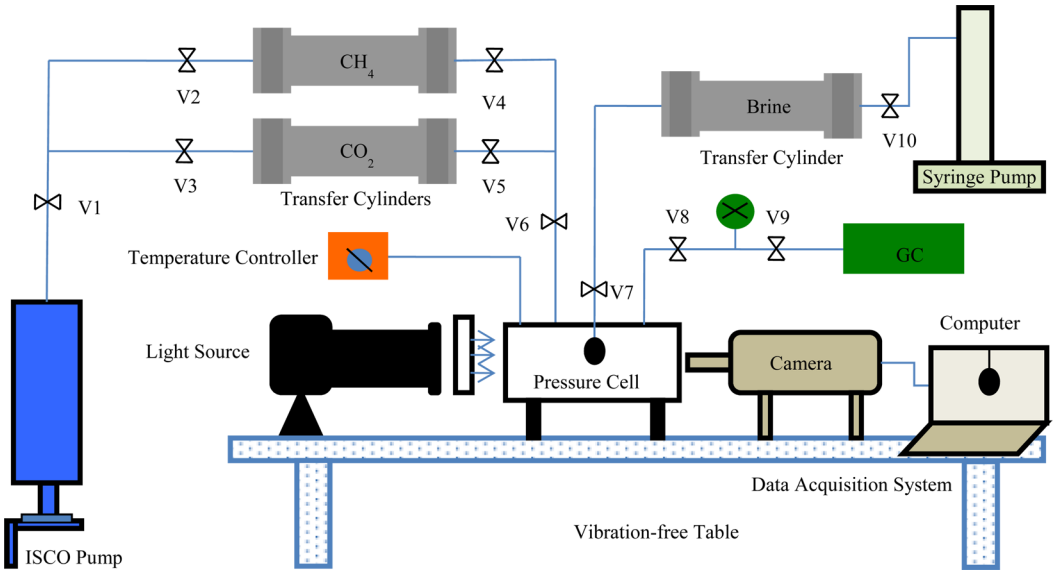

Figure 2. Schematic diagram of the experimental setup for measuring the equilibrium IFTs of CO_2/CH_4/brine systems using the ADSA technique for the pendant drop case.

Table 2. Physical Properties of the Three Components Used in the IFT Model

component	P_c, psia	T_c, °F	acentric factor	molecular weight	volume shift	parachor
CO_2	1069.9	87.89	0.225	44.01	−0.15400	78
CH_4	667.2	−116.59	0.008	16.04	−0.01478	77
H_2O	3197.8	705.47	0.344	18.02	0.23170	52

min were required for the system to reach an equilibrium state at given pressure and temperature.

After the pendant water drop was formed in the gas phase, its digital image was well-focused through the diffused light, acquired sequentially, and stored by the computer. For each digital water drop image, a standard grid image was used to calibrate the drop image and correct possible optical distortion. The ADSA program for the pendant drop case was then executed to determine the equilibrium IFT. The output data also included the radius of the curvature at the apex point, and the volume and surface area of the pendant water drop. Only the local gravitational acceleration and the gas−water density difference were required as the input data for this program. Knowing the pendant drop dimensions and the fluid densities enabled the calculations of IFT. During the IFT measurement, gas-phase and liquid-phase densities needed to be input into the software. In this study, as for CO_2/H_2O, CH_4/H_2O, and $CO_2/CH_4/H_2O$ systems, we calculated the densities of the liquid phase and vapor phase by an enhanced Peng−Robinson equation of state (PR EOS) model with temperature-dependent binary interaction parameters and constant volume shift parameters. More specifically, we used a new BIP correlation developed by Li and Yang[41] to estimate the BIP of CO_2/H_2O binary; this BIP correlation is a function of the reduced temperature of CO_2. Meanwhile, we used a BIP correlation developed by Søreide and Whitson[42] to estimate the BIP of CH_4/H_2O binary; this BIP correlation is a function of temperature and acentric factor of CH_4. Table 2 lists the physical properties of CO_2, CH_4, and H_2O used in the PR EOS model. As for CO_2/brine, CH_4/brine, and CO_2/CH_4/brine systems, in order to obtain an accurate phase density predictions, we used a modified PR EOS model by Søreide and Whitson[42] with constant volume shift parameters. This model considers salinity and mutual solubility of CH_4/brine and CO_2/brine binaries.

In this study, much care has been taken to eliminate possible error sources in IFT measurements. First, as recommended by the manufacturer, the settings for KRÜSS software suitable for gas−water IFT measurements were set as (light level = 2, brightness = 31, gain = 10, exposure = −11). Second, a steel needle with an outer needle diameter of 0.70 mm was used in the tests to control the droplet size. During the experiments, extra efforts were devoted to generating large droplets at the needle tip; larger droplet volumes created more accurate IFT measurements because the effect of the capillary tube tip diminished as the drop volume became larger.[43] In addition, all the IFT data were measured under equilibrium conditions.

3. MATHEMATICAL FORMULATION

Most of the previous IFT models originated from the Parachor model.[6,13,14,44−49] For example, Chalbaud et al.[6] developed a correlation on the basis of the Parachor model taking into account the influence of temperature, pressure, salt presence, and chemical structure of CO_2. Ayirala and Rao[49] proposed a new mechanistic Parachor model based on mass transfer to predict IFT in multicomponent hydrocarbon systems.

Sugden[50] proposed an equation including the new constant Parachor in the following form:

$$\sigma^{1/4} = \frac{P}{M}\Delta\rho \tag{1}$$

where σ is the IFT between two phases; P is Parachor; M is molecular weight of the component; and $\Delta\rho$ is density difference between two phases. Quayle[51] determined the Parachor for a large number of compounds considering their

DOI: 10.1021/acs.iecr.6b02446
Ind. Eng. Chem. Res. 2016, 55, 12358−12375

molecular structures. Weinaug and Katz[24] extended Sugden's equation[50] to mixtures as follows:

$$\sigma^{1/4} = \sum_{i=1}^{n} P_i\left(\frac{\rho_L}{M_L}x_i - \frac{P_V}{M_V}y_i\right) \quad (2)$$

where P_i is Parachor for component i; M_L is the average molecular weight of liquid phase; M_V is the average molecular weight of vapor phase; ρ_L is density of liquid phase; ρ_V is density of vapor phase; x_i is the mole fraction of component i in liquid phase; and y_i is the mole fraction of component i in vapor phase. The equation proposed by Weinaug and Katz[24] is used as a standard method of IFT prediction in the petroleum industry. It has been applied to some binary hydrocarbon systems and pure hydrocarbons successfully, but generally does not perform well for gas/water systems.[28]

Firoozabadi and Ramey[28] presented a correlation for estimating the IFT of hydrocarbon gas or hydrocarbon liquid with water. The phase density difference and reduced temperature for the hydrocarbon phase were chosen to be two correlating parameters. It correlates the IFT to the density difference between gas phase and liquid phase with an exponent of 4 based on the assumption from the van der Waals equation

$$\frac{\sigma_{hw}^{0.25}}{\rho_w - \rho_h}\left(\frac{T_{\circ R}}{T_c}\right)^{0.3125} = f(\Delta\rho) \quad (3)$$

where σ_{hw} is IFT between hydrocarbon and water, dyn/cm; ρ_w is pure water density, g/cm^3; ρ_h is density of hydrocarbon, g/cm^3; T_c is critical temperature of water, °R; and $T_{\circ R}$ is temperature, °R. One can plot the LHS of eq 3 with respect to phase density difference to find out their proper relationship. Danesh[4] presented a modified version of eq 3 for modeling IFT of hydrocarbon/water systems as

$$\sigma_{hw} = 111(\rho_w - \rho_h)^{1.024}\left(\frac{T_{\circ R}}{T_c}\right)^{-1.25} \quad (4)$$

where σ_{hw} is IFT between hydrocarbon and water, dyn/cm; ρ_w is pure water density, g/cm^3; ρ_h is density of hydrocarbon, g/cm^3; T_c is critical temperature, K; and $T_{\circ R}$ is temperature, °R.

Sutton[30] developed another empirical correlation for determining IFT of hydrocarbon-gas/water systems

$$\sigma_{gw} = \left[\frac{1.53988(\rho_{w_{g/cm^3}} - \rho_{h_{g/cm^3}}) + 2.08339}{\left(\frac{T_{\circ R}}{T_c}\right)^{(0.821976 - 1.83785\times10^{-3}T_{\circ R} + 1.34016\times10^{-6}T_{\circ R}^2)}}\right]^{3.6667} \quad (5)$$

where σ_{gw} is IFT between gas and water, dyn/cm; $\rho_{w_{g/cm^3}}$ is density of water phase, g/cm^3; and $\rho_{h_{g/cm^3}}$ is density of the hydrocarbon-gas phase, g/cm^3; $T_{\circ R}$ is temperature, °R; T_c is the critical temperature of water, °R. As pointed out by Chalbaud et al.,[22] Firoozabadi and Ramey's correlation[28] might not be applicable to some gases, such as CO_2, because the gas solubility in water can be large.

All of the correlations mentioned above were developed based on the IFT measurements and the phase density difference between hydrocarbon gases with water. From our experimental results, we observed that the IFT of gas mixtures with water has a strong correlation with gas composition in addition to the effect of temperature, pressure, and density difference. Considering these factors, we present a new IFT correlation

$$\left(\frac{\sum_{i=1}^{n} z_i M_i}{M_H}\right)^{0.183361} \frac{\sigma_{gw}^{0.25}}{(\rho_M^L \sum_{i=1}^{n} x_i P_i - \rho_M^V \sum_{i=1}^{n} y_i P_i)} T_r^{0.3125} = f(\rho_M^L \sum_{i=1}^{n} x_i P_i - \rho_M^V \sum_{i=1}^{n} y_i P_i) \quad (6)$$

where z_i is the overall mole fraction of component i in the gas phase; M_i is molecular weight of component i, g/mol; M_H is the molecular weight of the heaviest component in the gas mixture, g/mol; T_r is reduced temperature of water; ρ_M^L is molar density of liquid phase, mol/m^3; ρ_M^V is molar density of vapor phase, mol/m^3; x_i is mole fraction of component i in liquid phase; and y_i is mole fraction of component i in vapor phase. This correlation takes into account the effects of pressure, temperature, individual compound's molecular weight, density difference, and gas composition on on IFT of gas-mixtures/water systems.

Also, at the same temperature and pressure, a different IFT can be found for a given gas mixture due to different water salinities. Argaud[29] presented a comprehensive review on salt's effect on IFT. Many scholars, such as Chalbaud et al.,[6] Argaud,[29] and Massoudi and King,[12] have found that there exists a unique linear relationship between IFT increment and the salt concentration of NaCl; and the slope of this line is independent of temperature when a IFT plateau is reached. Analogous to previous works (such as that of Standing[52]), a linear relationship between IFT increment for CO_2/brine and CH_4/brine systems and the salt (NaCl) concentration is also provided as follows:

$$\sigma_{cor} = kC_s \quad (7)$$

where σ_{cor} represents the increase in IFT due to salinity effect, mN/m; and C_s represents the molar concentration of salt in water, mol/kg; and k is regression constant.

In this study, we find that the salt (NaCl) effects on IFT of the CO_2/brine and CH_4/brine systems are different from each other, although a linear relationship holds between IFT increment and NaCl concentration for both systems. The IFT of a given CO_2/CH_4/brine system can be determined by first calculating the IFT for CO_2/CH_4/water systems and then applying the following correction:

$$\sigma_{gb} = \sigma_{gw} + y_{CH_4}\sigma_{cor-CH_4} + y_{CO_2}\sigma_{cor-CO_2} \quad (8)$$

where σ_{gb} represents IFT between gas and brine; σ_{gw} represents IFT between gas and pure water; σ_{cor-CH_4} represents the increase in IFT due to salinity effect for CH_4/brine system, mN/m; σ_{cor-CO_2} represents the increase in IFT due to salinity effect for CO_2/brine system, mN/m; y_{CH_4} is the mole fraction of CH_4 in the original gas mixture; and y_{CO_2} is the mole fraction of CO_2 in the original gas mixture.

4. RESULTS AND DISCUSSION

4.1. Comparison with Published Data. In order to validate the reliability of IFT measurements made in this study, IFTs measured at 80.0, 81.0, 163.0, and 257.0 °F for CO_2/H_2O and CH_4/H_2O systems are compared with the published data given in Table 1. Figures 3−8 show the IFTs measured in this

DOI: 10.1021/acs.iecr.6b02446
Ind. Eng. Chem. Res. 2016, 55, 12358−12375

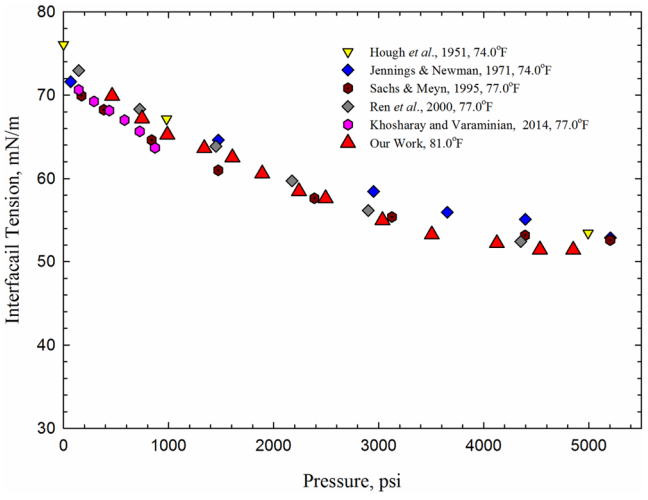

Figure 3. Comparison of CH_4/H_2O IFTs measured in this study at 81.0 °F and IFTs measured previously over 74.0−81.0 °F.

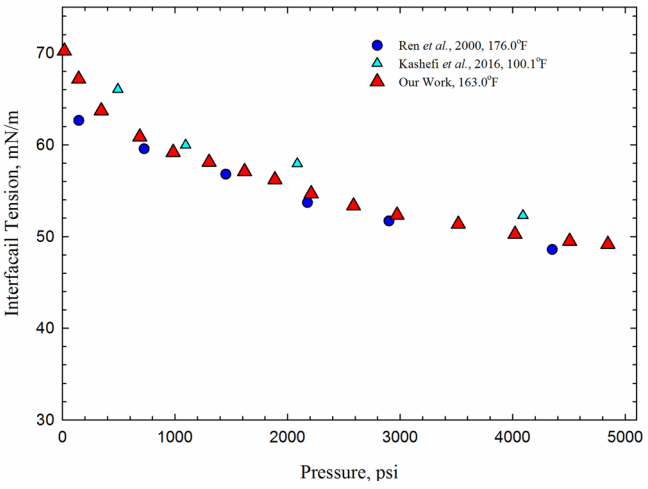

Figure 4. Comparison of CH_4/H_2O IFTs measured in this study at 163.0 °F and IFTs measured previously over 100.1−176.0 °F.

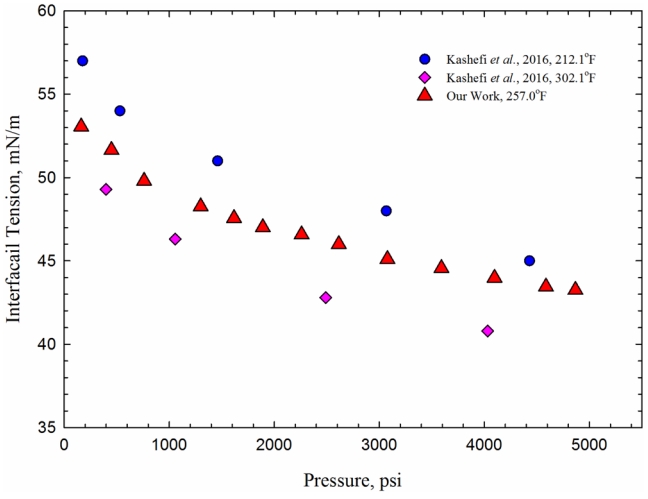

Figure 5. Comparison of CH_4/H_2O IFTs measured in this study at 257.0 °F and IFTs measured previously over 212.1−302.1 °F.

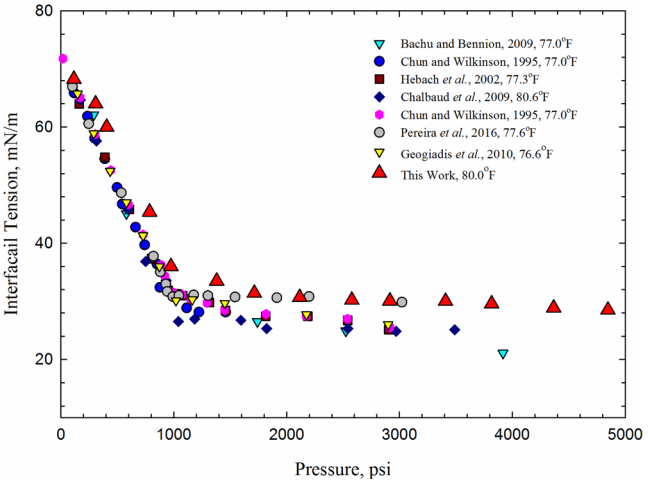

Figure 6. Comparison of CO_2/H_2O IFTs measured in this study at 80.0 °F and IFTs measured previously over 76.6−80.6 °F.

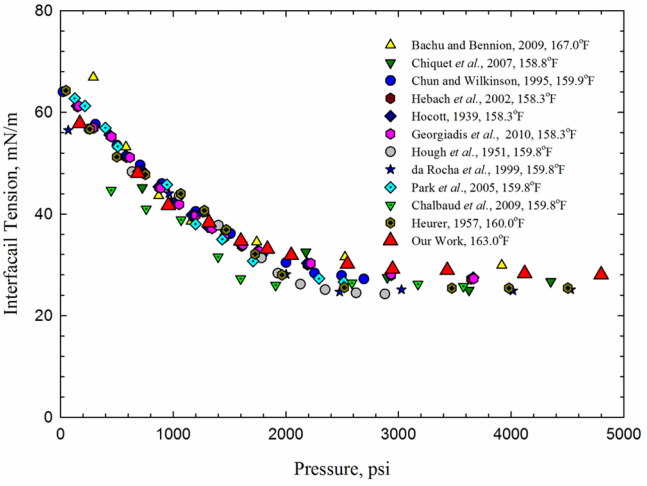

Figure 7. Comparison of CO_2/H_2O IFTs measured in this study at 163.0 °F and IFTs measured previously over 158.3−167.0 °F.

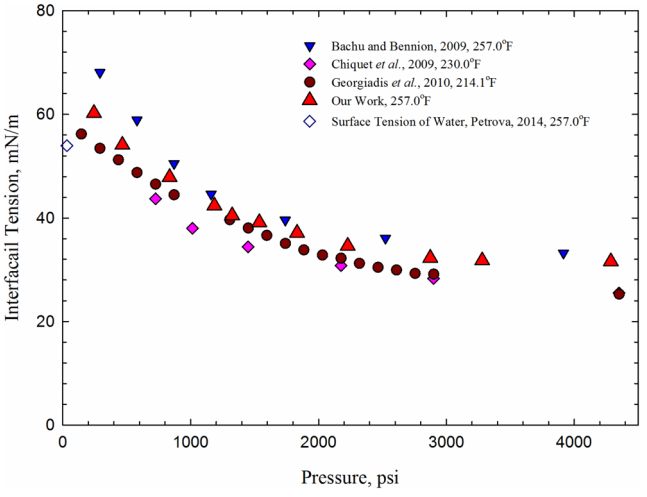

Figure 8. Comparison of CO_2/H_2O IFTs measured in this study at 257.0 °F and IFTs measured previously over 214.1−257.0 °F.

study, together with those measured previously at or close to these temperatures. For all plots, the color-filled (other than red) symbols represent published data, while the red-filled triangles are IFTs measured in this study. Figures 3−5 compare the IFT of CH_4/H_2O systems measured in this study with the

DOI: 10.1021/acs.iecr.6b02446
Ind. Eng. Chem. Res. 2016, 55, 12358−12375

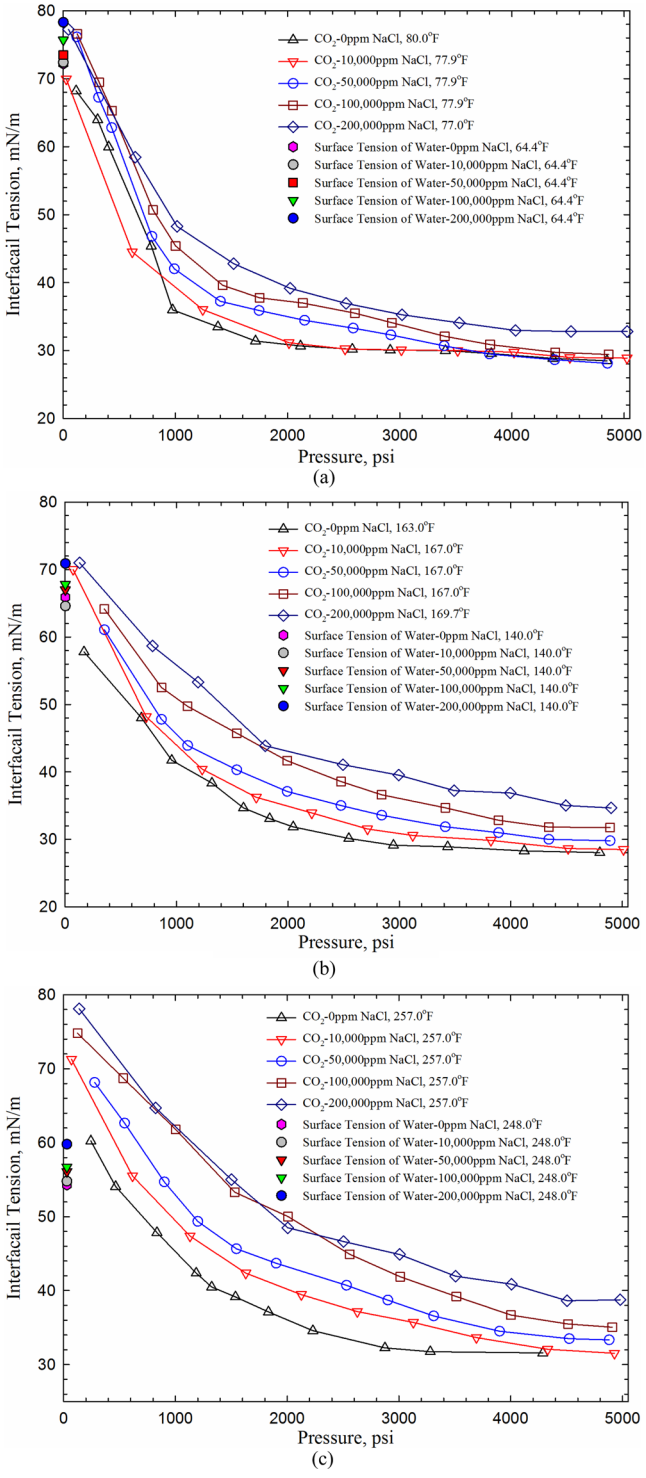

Figure 9. IFT of CO_2/brine system as a function of pressure at different temperatures and different salinities. The surface tension of brine was measured by Abramzon and Gaukhberg.[73]

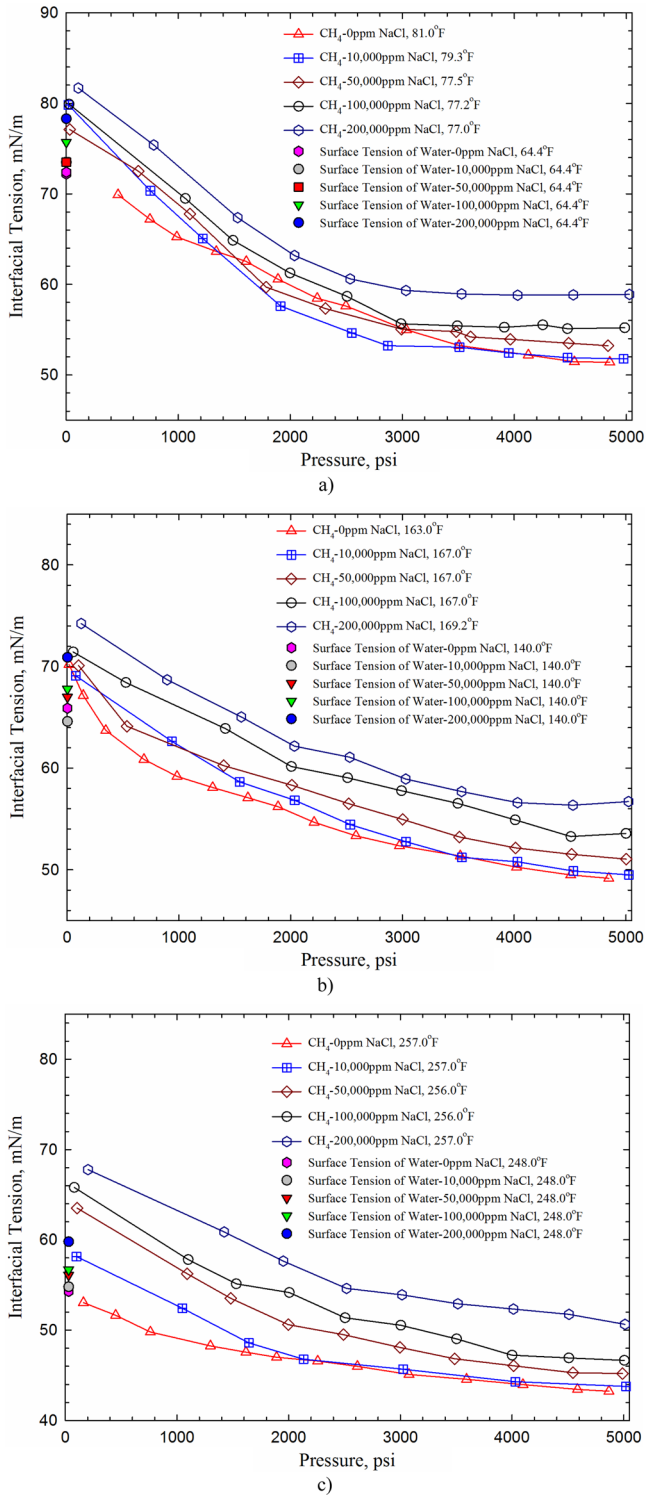

Figure 10. IFT of CH_4/brine system as a function of pressure at different temperatures and different salinities. The surface tension of brine was measured by Abramzon and Gaukhberg.[73]

published data by Hough et al.,[53] Jennings and Newman,[54] Sachs and Meyn,[55] Ren et al.,[11] Khosharay and Varaminian,[56] and Khashefi et al.[15] It can be seen from Figures 3−5 that our measurement results for CH_4/H_2O systems are comparable to the published data. Our IFT data deviate much from those of Hocott.[57] This is because Hocott[57] used a gas phase that was dominated by CH_4 but also contained a small amount of C_2H_6 and C_3H_8. Figures 6−8 shows the comparison of IFTs of CO_2/H_2O systems measured in this study against the published IFT data by Hocott,[57] Hough et al.,[53] Heuer,[58] Chun and Wilkinson,[59] da Rocha et al.,[60] Hebach et al.,[31] Park et al.,[61] Chiquet et al.,[62] Bachu and Bennion,[21] Chalbaud et al.,[22] and Georgiadis et al.[63] When pressure is low enough or equal to the saturation pressure of the aqueous phase, the water/gas IFT data should approach the surface tension of water at zero

DOI: 10.1021/acs.iecr.6b02446
Ind. Eng. Chem. Res. 2016, 55, 12358−12375

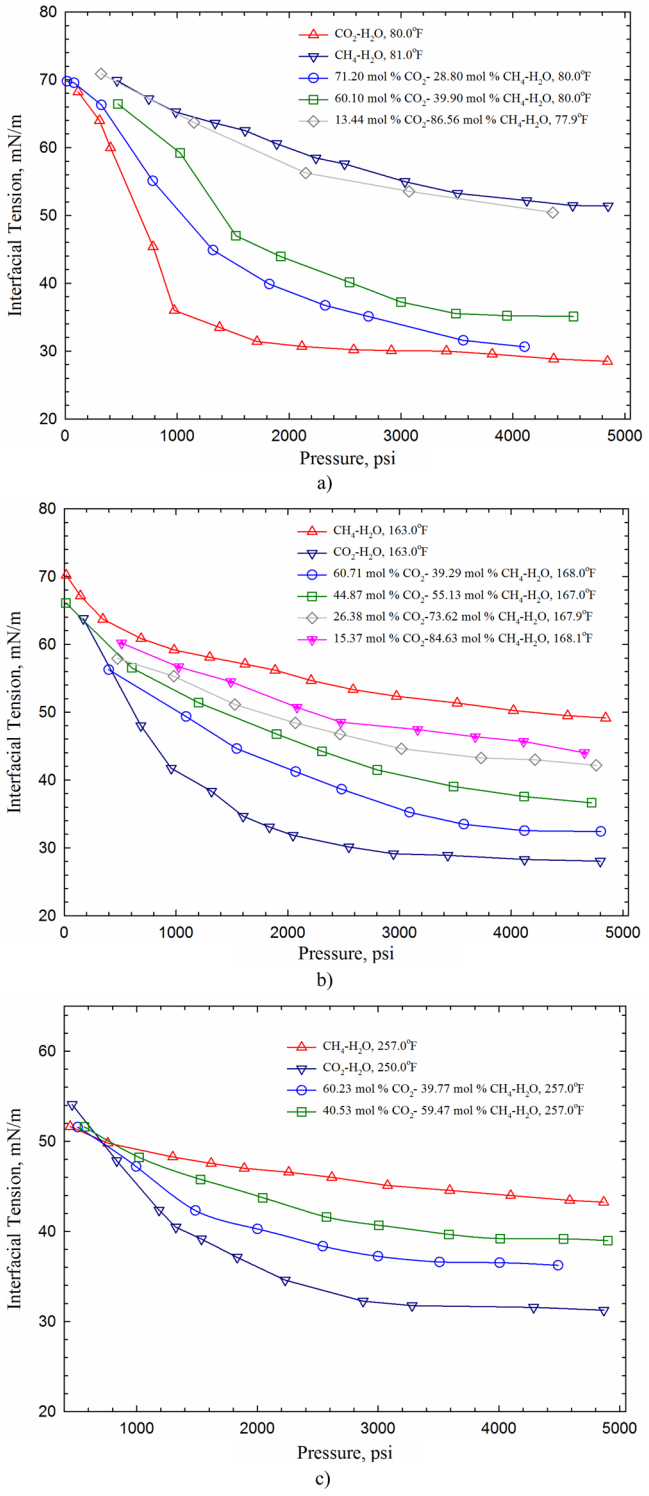

Figure 11. IFT of $CO_2/CH_4/H_2O$ systems as a function of pressure at different temperatures.

pressure and the temperature of interest. It has been found the surface tension of ordinary water at 257.0 °F is 53.96 mN/m,[64] as shown in Figure 8. The previous published and our measured IFT data deviate slightly from the constraint. This deviation may be caused by water vaporization at high temperatures.

4.2. Effect of Pressure, Temperature, and Salinity on IFT. In this section, we use the IFT measured for CO_2/brine (0−200 000 ppm of NaCl) (Figure 9) and CH_4/brine (0−200 000 ppm of NaCl) (Figure 10) at around 78.0, 167.0, and 257.0 °F, respectively, to analyze the effect of pressure, temperature, and salinity on IFT. Figure 9 presents the IFT isotherms of CO_2/brine system. It indicates that, at low pressures (below around 580.2−725.2 psia), IFTs decrease approximately linearly with increasing pressure at these three temperatures, corresponding to the so-called Henry regime.[62] Passing the Henry regime, pressure increase has less effect on the IFT reduction. When pressure increases to a high value, IFT levels off. In general, IFTs for CH_4/brine system are found to decrease with increasing temperature as shown in Figure 10. On the contrary, IFTs for CO_2/brine systems measured at higher temperatures are generally higher than those measured at lower temperatures. It is because the solubility of CO_2 in water varies significantly with temperature.[20] At a higher temperature, the solubility of CO_2 in water or brine is less than that at a lower temperature.[65−67] As salinity increases, the solubility of CO_2 in brine decreases, leading to changes in the brine density and IFT. As seen from Figure 9, the IFT of CO_2/brine systems exhibits a more pronounced reduction with an increase in pressure at a lower temperature than that at a higher temperature. The plateau for CO_2/brine system is reached at about 1400 psia at 78.0 °F, about 2000 psia at 167.0 °F, and about 2900 psia at 257.0 °F, respectively.

The salinity of brine in shale formations can be quite high, up to 300 000 ppm.[68] Salts can affect the interfacial tension between gas and water. When ions dissolve into liquid water, electrostatic force from ions can change the original structure of water, usually forming water molecular layer around ions which is called "hydration". Indeed, water will always stride to maintain its hydrogen-bonded structure in order to maintain thermodynamic stability, while salts can affect such bonded structure formed by water, and thus affect the IFT between gas and water. In this study, IFT measurements are conducted at salinities up to 200 000 ppm of NaCl for both CO_2/brine and CH_4/brine systems, as shown in Figures 9 and 10. Similar to CH_4/H_2O and CO_2/H_2O systems, the IFT of CH_4/brine and CO_2/brine systems exhibits a decreasing trend with increasing pressure at a given temperature. Furthermore, at the same temperature, IFT increases as more NaCl is present in water. This is attributed to the fact that, as salinity increases, the specific gravity of brine also increases; this enlarges the density difference between gas phase and liquid phase, leading to a higher IFT of the gas/brine system. At lower pressures, the IFTs corresponding to different salinities usually cross with each other in the range of 15.0−725.2 psia. Such crossing behavior might be related to the complex gas solubility in liquid phase at different temperatures.[20] Chalbaud et al.[6] presented when NaCl concentration is lower than 5,000 ppm, salinity effect on IFT is negligible. For CO_2/brine systems at a low pressure, salinity shows a more obvious effect on IFT, while the salt effect on IFT reaches to a given value as the pressure becomes higher. Meanwhile, at high pressures, the average IFT increment for different NaCl concentrations depends on neither pressure nor temperature. Some scholars[69,70] measured the solubility of CO_2 in water and brine as a function of pressure. They attributed the existence of a plateau to the solubility effect on the IFT reduction. Meanwhile, some studies[69−71] presented that the pressure-dependence of CO_2 solubility in brine exhibits a similar trend to that in pure water.

Our measurements were limited to the conditions of 77.0−257.0 °F and 15−5050 psia. Wiegand and Franck[72] measured

DOI: 10.1021/acs.iecr.6b02446
Ind. Eng. Chem. Res. 2016, 55, 12358−12375

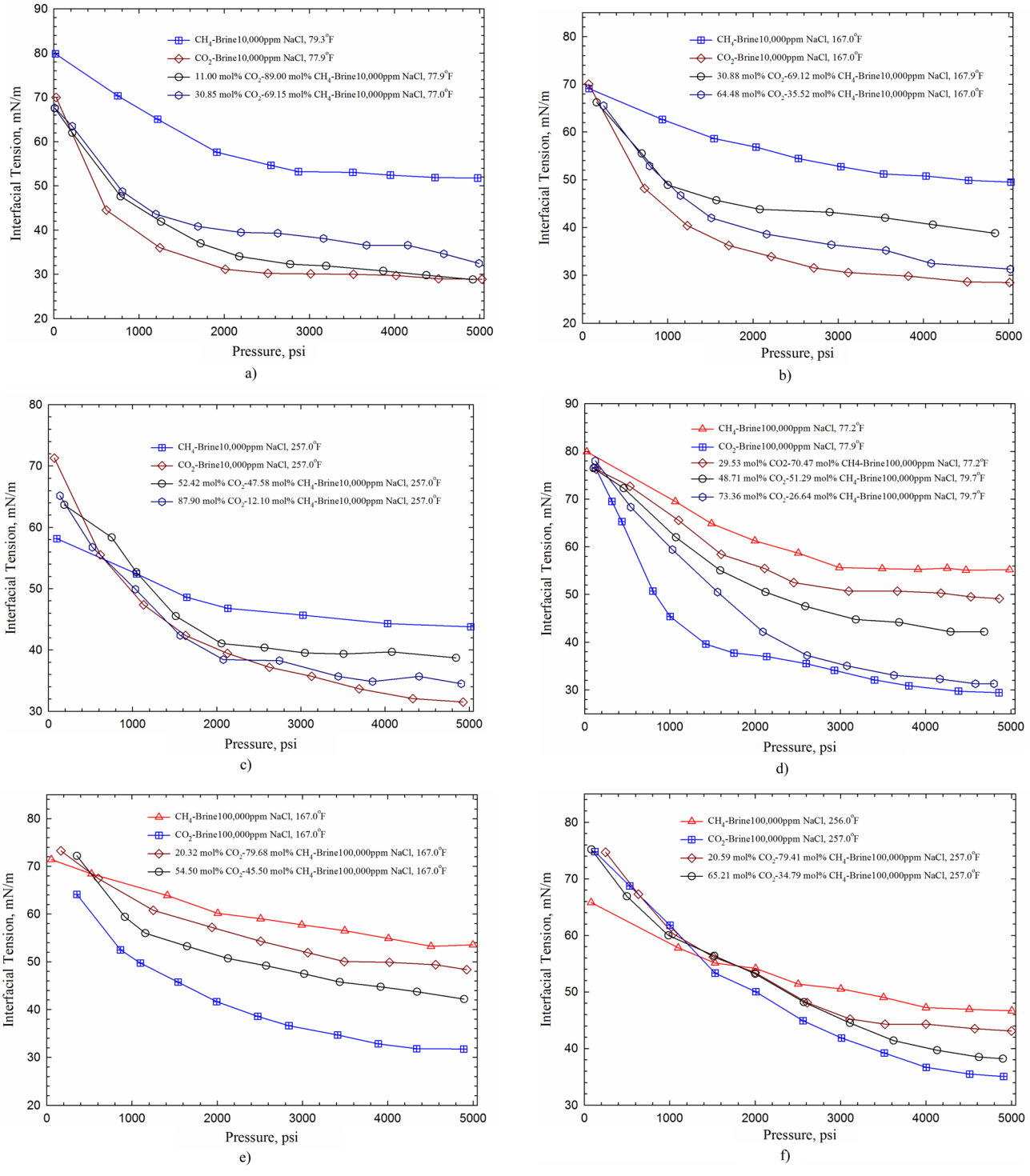

Figure 12. continued

DOI: 10.1021/acs.iecr.6b02446
Ind. Eng. Chem. Res. 2016, 55, 12358−12375

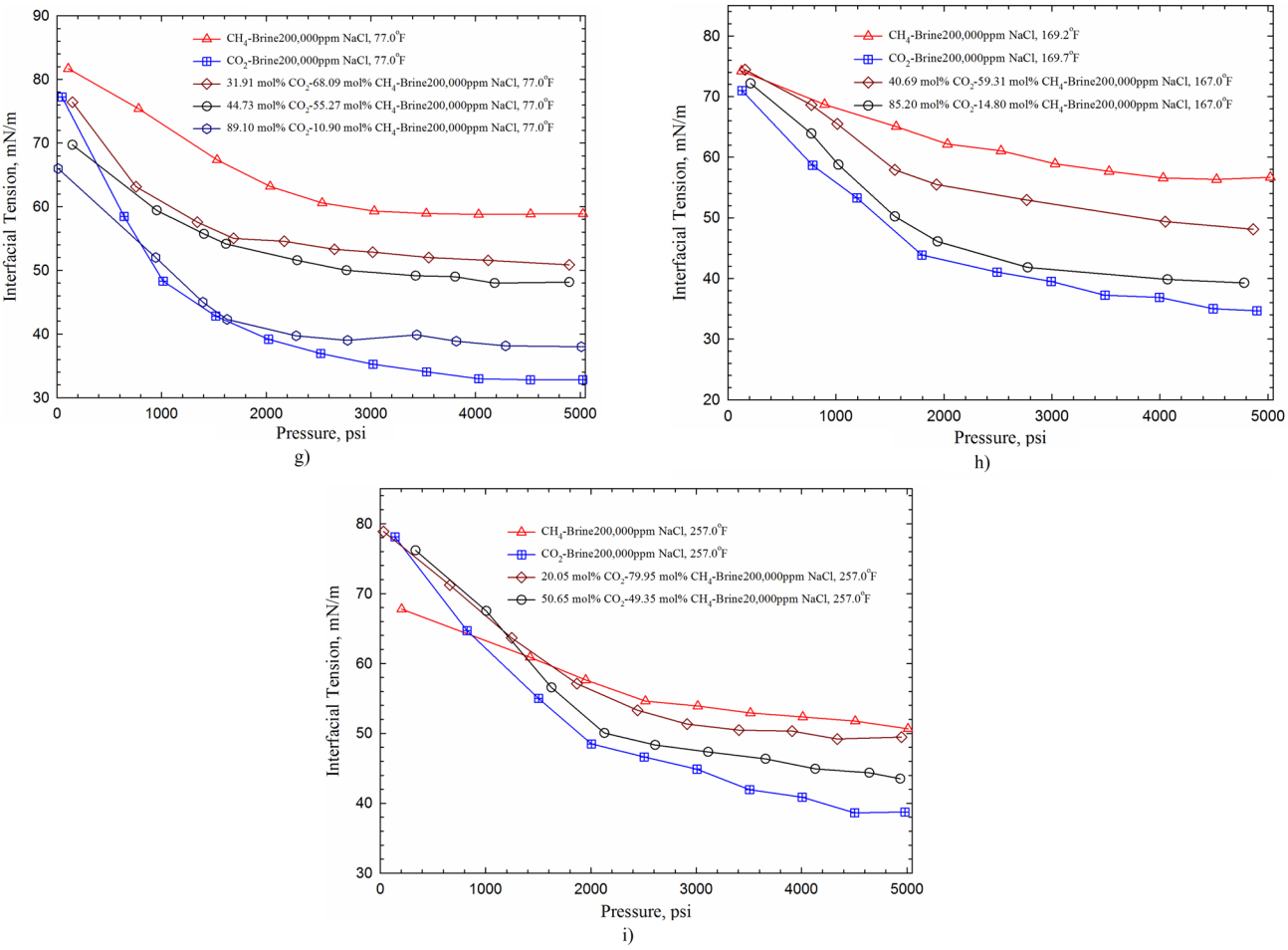

Figure 12. IFT of CO_2/CH_4/brine as a function of pressure at different temperatures and NaCl concentrations.

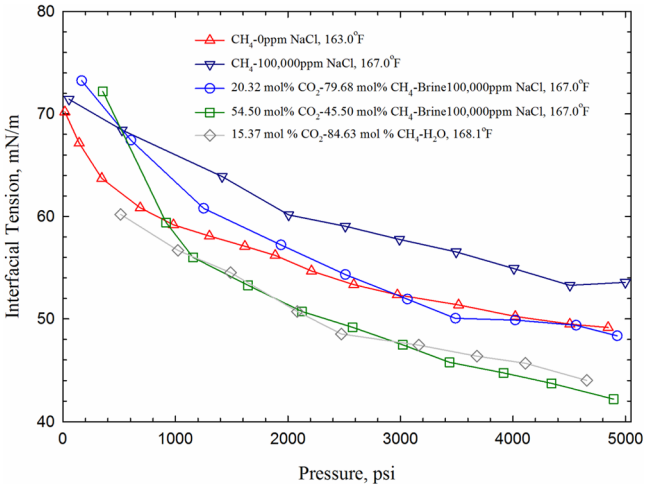

Figure 13. IFT of CH_4/CO_2/brine systems as a function of pressure.

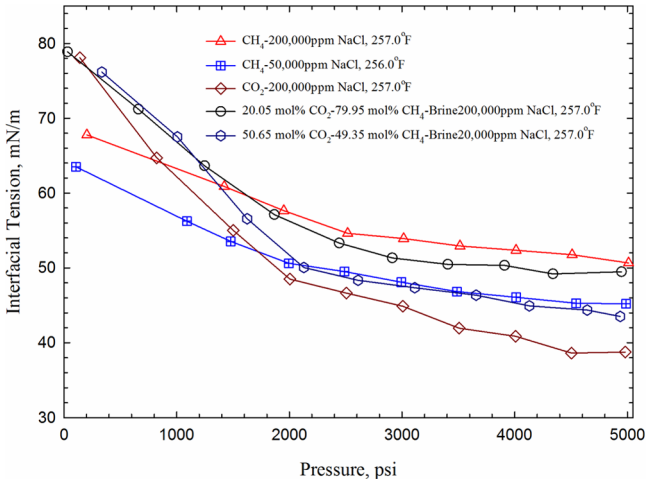

Figure 14. IFT of CO_2/CH_4/brine systems as a function of pressure.

the IFT of various gases and water systems covering much greater temperature and pressure ranges. They found the IFT levels off when pressure exceeds 2175.6−2900.8 psia, while it increases very slowly with pressures above 7251.9−14503.8 psia.

Regarding the IFT results of the CH_4/brine system as shown in Figure 10, similar conclusions can be made. The CH_4/brine IFT also decreases with an increasing pressure until it reaches at a plateau. At the same temperature, CH_4/brine system needs a higher pressure to reach the plateau compared to a CO_2/brine system. At about 81.0 °F, for example, the value of the plateau is reached at about 2800 psia, and about 4000 psia at 163.0 °F. Figures 9 and 10 indicate that the CH_4/brine IFT is overall higher than that of CO_2/brine. The physical properties of CH_4 and CO_2 cause such difference; CH_4 has a lower solubility in water compared with CO_2 at the same temperature and pressure. Also, at the same pressure and temperature, the

DOI: 10.1021/acs.iecr.6b02446
Ind. Eng. Chem. Res. 2016, 55, 12358−12375

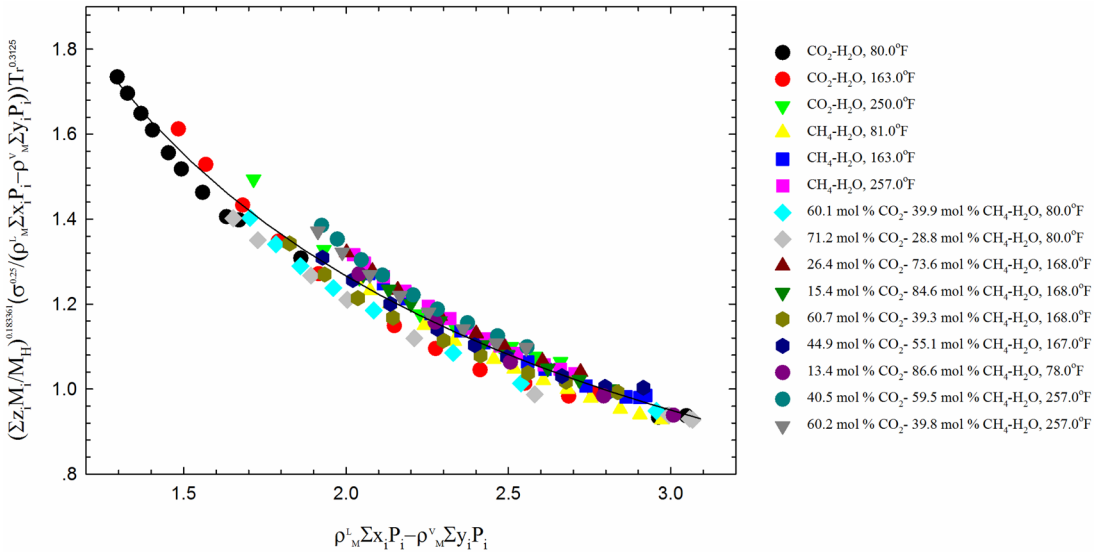

Figure 15. Regression of IFT model parameters using measured data in this study for $CO_2/CH_4/H_2O$ systems.

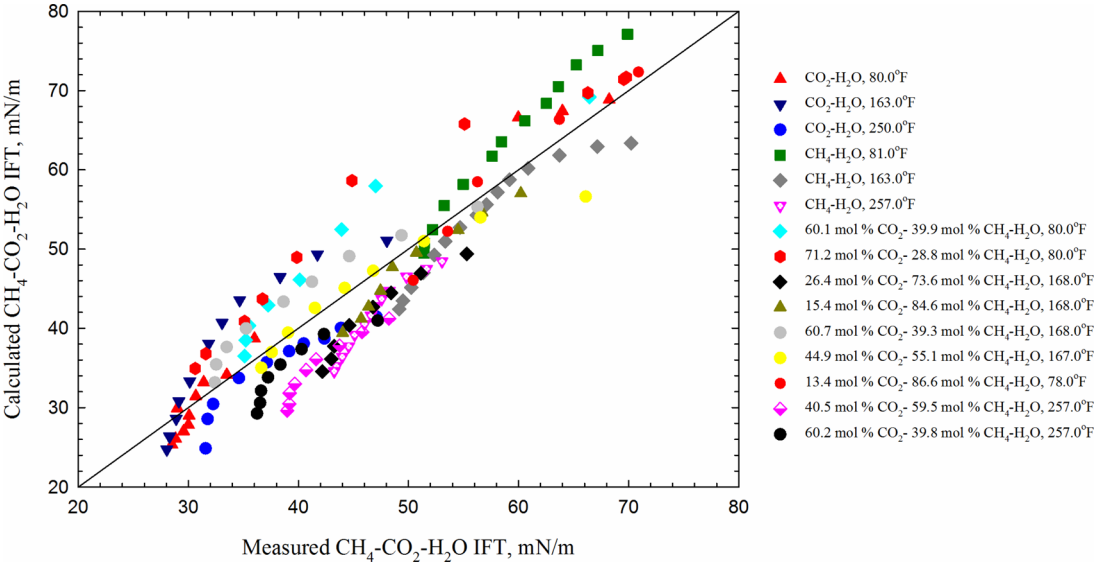

Figure 16. Comparison between predicted IFTs with eq 9 versus measured IFTs for $CO_2/CH_4/H_2O$ systems.

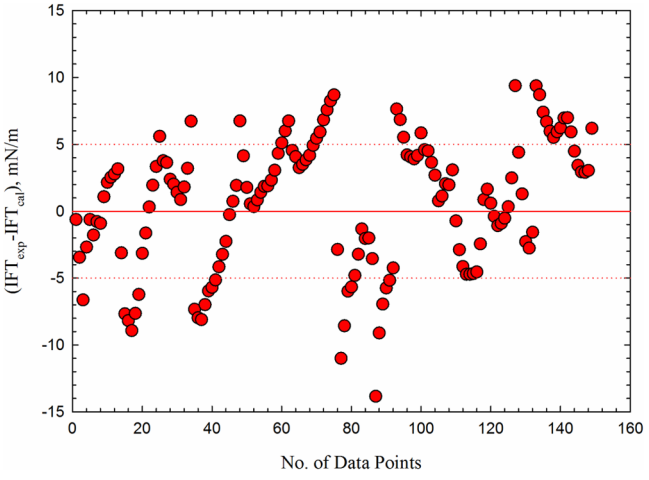

Figure 17. Difference between measured IFTs and predicted IFT with eq 9 for $CO_2/CH_4/H_2O$ systems.

Table 3. Performance of Different IFT Models in Reproducing the IFTs of $CO_2/CH_4/H_2O$ Systems

model	number of data points obtained by this study	AARE, %	SD, %
new model	156	9.42	11.33
Danesh et al.[4] 1998	156	28.28	38.48
Sutton[30] 2009	156	23.13	40.39
Firoozabadi and Ramey[28] 1988	156	25.52	29.08
Weinaug and Katz[24] 1943	156	35.98	44.11

density difference between gas phase and liquid phase of the CH_4/brine system is larger than that of the CO_2/brine system.

As for the IFT between gas and brine, when pressure is low enough or equal to the saturation pressure of the aqueous phase, the brine/gas IFT data should approach the surface tension of water at zero pressure and the temperature of interest. The surface tensions of ordinary brine at different

DOI: 10.1021/acs.iecr.6b02446
Ind. Eng. Chem. Res. 2016, 55, 12358−12375

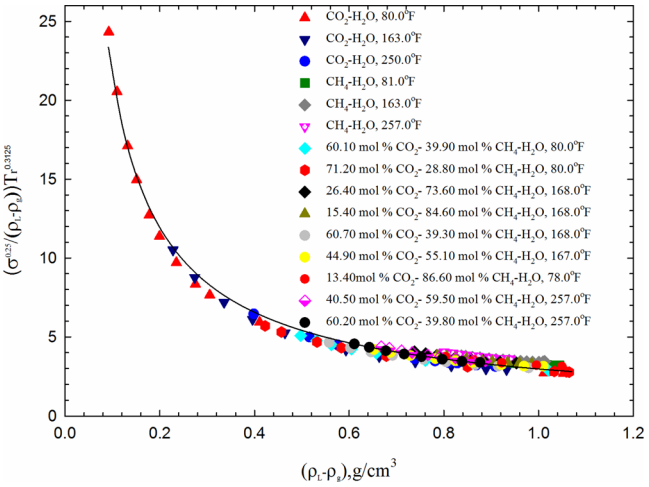

Figure 18. Application of Firoozabadi and Ramey[28] correlation to the IFT data of $CO_2/CH_4/H_2O$ systems.

temperatures were measured by Abramzon and Gaukhberg;[73] these surface tensions have been labeled in Figures 9 and 10.

For the experimental surface tension of salt solutions measured by Abramzon and Gaukhberg,[73] we assumed that the surface tensions were measured at the saturation pressure of a specific salt solution because no specific operating pressures were reported in the paper. From Figures 9 and 10, this constraint is only satisfied at 77.0 °F. However, at 167.0 °F and at atmospheric pressure, the experimental IFTs tend to be higher than the brine surface tension. This can be explained as follows. At 77.0 °F, the brine drop in the IFT cell can maintain as a single liquid phase because water's saturation pressure at 77.0 °F is lower than the atmospheric pressure. Therefore, the reported gas/brine IFT data should tend to be the exact brine surface tension at this temperature. However, at higher temperatures (such as 167.0 °F), water molecules are more apt to escape form liquid phase into vapor phase, which leads to a higher salinity of the brine drop and also causes a larger density difference between the liquid phase and vapor phase. Hence, relatively higher IFTs could be resulted at higher temperatures.

When the temperature is higher than the saturation temperature at atmospheric pressure, such as 257.0 °F, the drop cannot maintain as a single liquid phase, but vapor phase. In the literature, surface tensions of brine or pure water reported at higher temperatures mostly were measured using the differential maximum bubble pressure method.[74] For this method, a bubble chamber unit is applied, leading to a curved interface between gas and liquid phases. There may be a permanent state of metastability because of the negative pressure effect when the gas–liquid interface is curved.[75] As shown in Figures 8, 9c, and 10c, the deviation persists at higher temperatures; this may arise from the effect of water vaporization, as mentioned above.

4.3. Effect of CO_2 Concentration on IFT. Supercritical CO_2 can be used as hydraulic fracturing fluid or enhanced gas recovery medium in shale reservoirs. Investigation on the CO_2 addition on IFT of CH_4/brine system is important for understanding the multiphase fluid flow within both the fracture and matrix. Figures 11 and 12 show the measurement results at different temperatures. The detailed data shown in Figures 11 and 12 are given in the Supporting Information (see Tables S1 and S2). It can be seen that the presence of CO_2 in CH_4 leads to reduction in IFT between gas mixtures and brine. A lower IFT can be expected if CO_2 is added into the gas phase, but the degree of IFT reduction depends on the amount of CO_2 added. With more CO_2 present in the gas mixture, the IFT reduction effect is more pronounced. As shown in Figure 11b, the IFT reduction ratio is more than 25% for the CH_4/H_2O system with 44.87 mol % CO_2 added at 163.0 °F. Similarly, in Figures 12a and f, the IFT reduction for the CH_4/brine systems is pronounced even at low concentrations of CO_2. The density difference between gas phase and liquid phase is reduced if CO_2 is added to CH_4, which is a major factor causing IFT reduction. Another reason is because CO_2 exhibits a higher solubility in water or brine compared to CH_4, further decreasing the density difference. The phase behavior of CO_2/CH_4 mixture with water or brine, together with the physical properties of the gas components, all contribute to the IFT reduction effect.

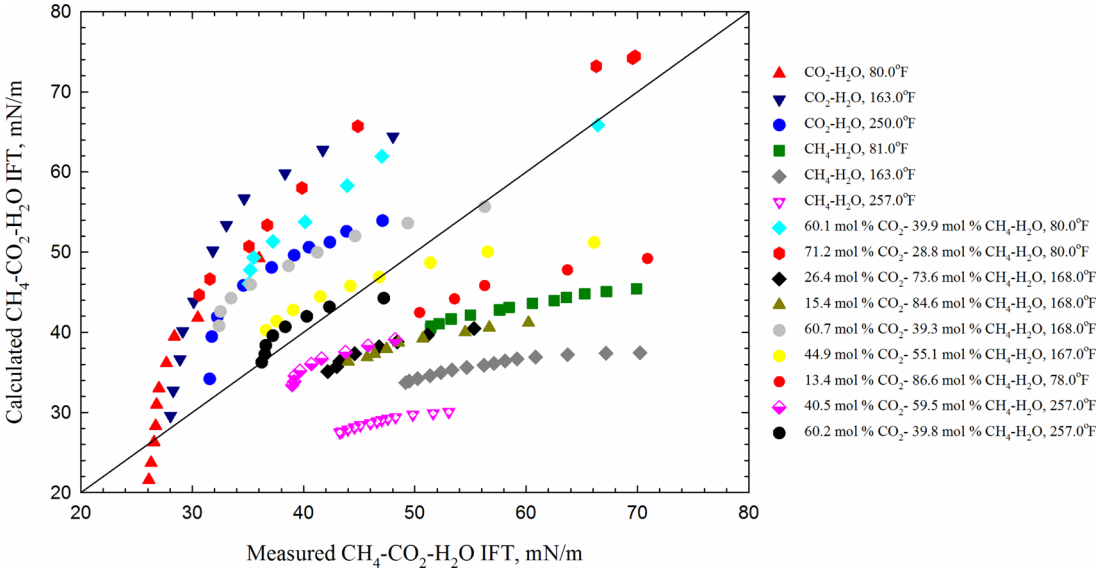

Figure 19. Comparison between the measured IFTs and calculated ones with the Firoozabadi and Ramey[28] correlation for $CO_2/CH_4/H_2O$ systems.

DOI: 10.1021/acs.iecr.6b02446
Ind. Eng. Chem. Res. 2016, 55, 12358–12375

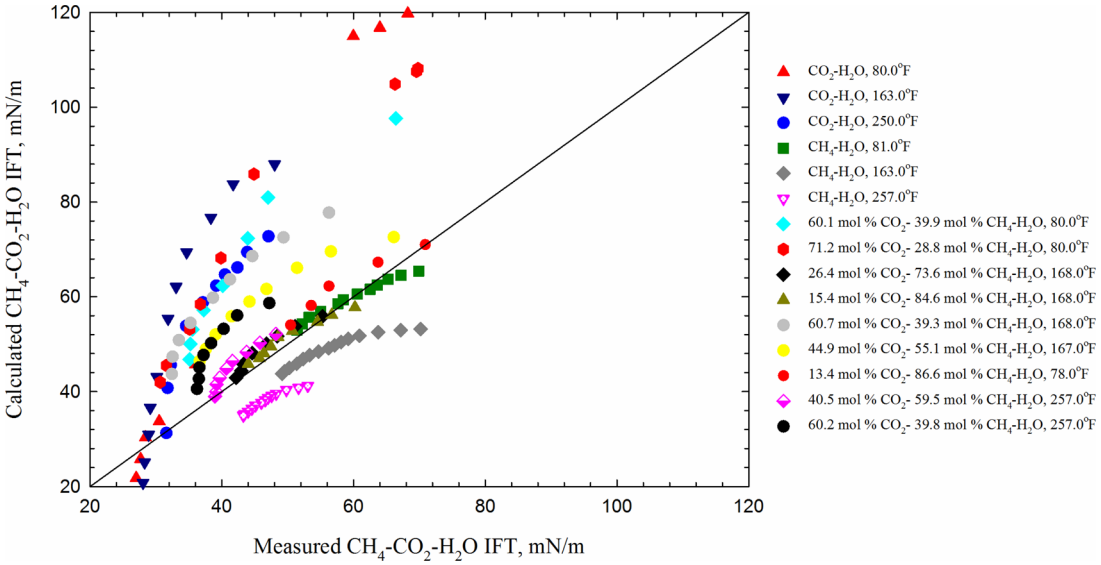

Figure 20. Comparison between the measured IFTs and calculated ones with the Danesh[4] correlation for $CO_2/CH_4/H_2O$ systems.

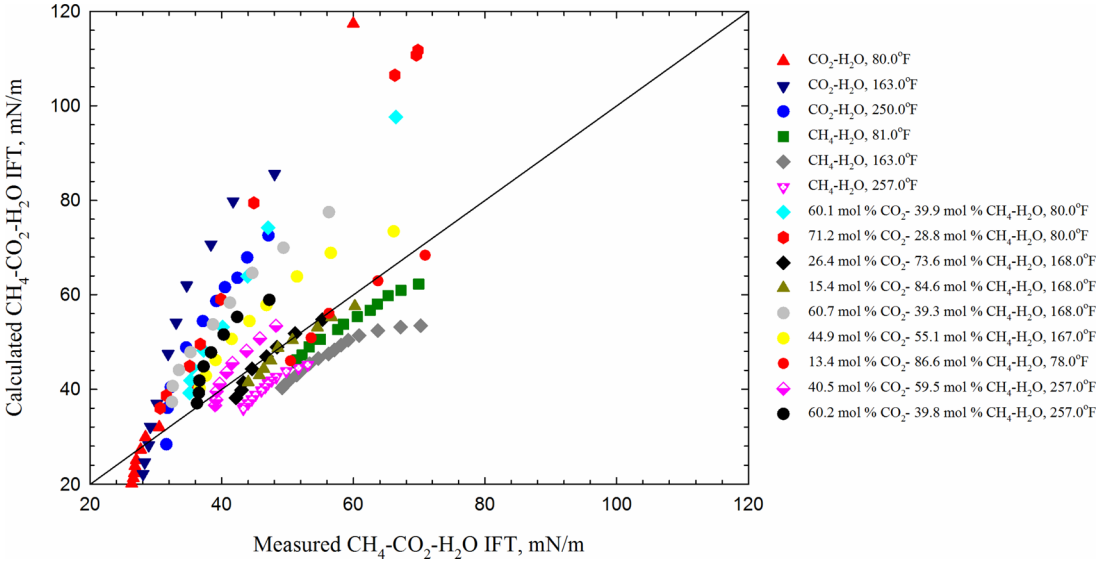

Figure 21. Comparison between the measured IFTs and calculated ones with the Sutton[30] correlation for $CO_2/CH_4/H_2O$ systems.

Rushing et al.[76] measured the effect of CO_2 concentration (up to 20.00 mol %) on IFT of gas−water system (gas CH_4 with a small fraction of C_2H_6 and C_3H_8) at high pressure−temperature conditions. They suggested that a higher concentration of CO_2 resulted in a lower IFT over a much greater pressure range than that for gases with lower CO_2 concentrations. They found that CO_2 concentration in vapor phase tended to decrease IFT of CH_4/brine systems at lower pressures, but slightly increased the IFT or showed no effect at higher pressures. It is, however, shown in our study that the presence of CO_2 has a significant effect on the IFT at both high and low pressures. Shariat[43] measured IFT for gas mixtures containing up to 20.00 mol % CO_2 (or without CO_2) with water over a wider pressure range, showing that the presence of CO_2 up to 20.00 mol % in gas mixtures has no significant effect on gas−water IFTs at higher pressures. Ren et al.[11] measured the IFT of $CO_2/CH_4/H_2O$ systems with CO_2 concentrations of 0, 20.00, 40.00, 60.00, and 80.00 mol % at temperatures of 104.0, 140.0, 176.0, and 212.0 °F, respectively. They found that CO_2 concentration of 20.00 mol % leads to negligible IFT reduction, and CO_2 concentrations of 20.00−40.00 mol % lead to minor reduction in IFT. They also reported IFT reduction at higher concentrations of CO_2 in gas mixture for all temperatures. However, we observed pronounced IFT reduction even at low CO_2 concentrations in our study.

The aforementioned experimental results demonstrate that CO_2 decreases the IFT of CH_4/H_2O systems, while salinity tends to increase the IFT of CH_4/H_2O systems. These IFT data are useful for assessing the engineering soundness of either using CO_2 for fracturing shale formations or CO_2 huff-and-puff for enhancing shale gas recovery. For a given shale reservoir, if the reservoir conditions such as reservoir temperature, pressure and salinity of formation water are given, the IFT between shale gas (mainly CH_4) and brine can be approximately determined.

Taking reservoir conditions, 167.0 °F and 4,351 psia, for example, the IFT between shale gas (mainly CH_4) with brine (with a salinity of 100 000 ppm of NaCl) is about 54.50 mN/m, about 4.00 mN/m higher than that of CH_4/H_2O system (see

DOI: 10.1021/acs.iecr.6b02446
Ind. Eng. Chem. Res. 2016, 55, 12358−12375

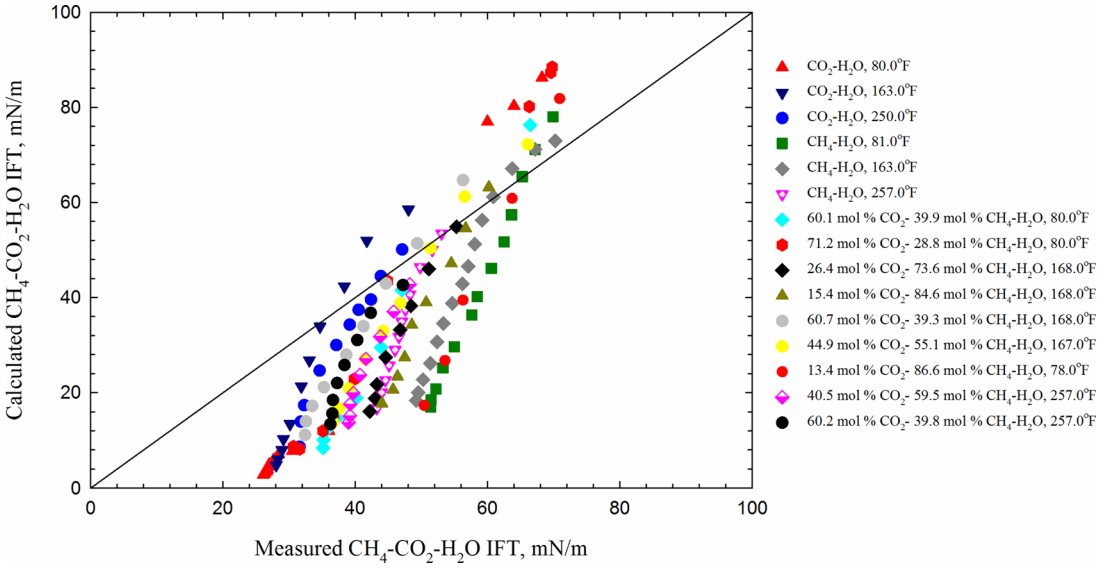

Figure 22. Comparison between the measured IFTs and predicted ones with the Weinaug and Katz[24] correlation for $CO_2/CH_4/H_2O$ systems.

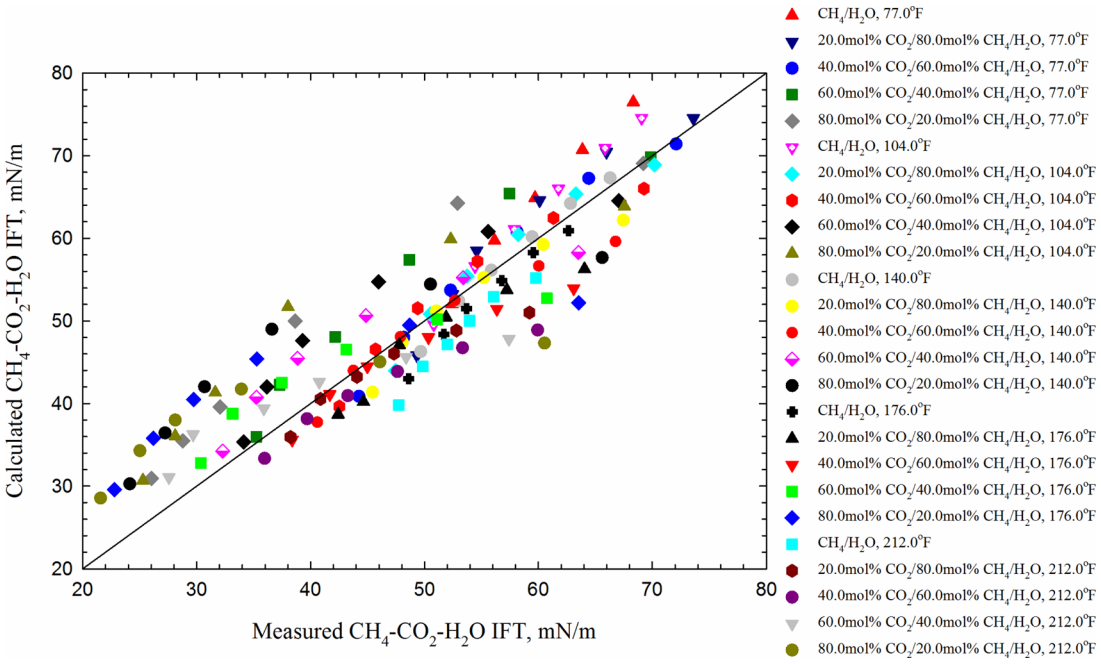

Figure 23. Comparison between the measured data by Ren et al.[11] and predicted IFTs with the new correlation for $CO_2/CH_4/H_2O$ systems.

Figure 13). IFT significantly affects the in situ capillary pressure and entrapment of gas in shale matrix; in order to enhance the shale gas recovery, gas/water IFT should be as low as possible. To reduce the IFT of CH_4/brine (with a salinity of 100 000 ppm of NaCl) system to a value of 45.50 mN/m, CO_2 concentration in the gas has to be around 50.00 mol %. Similarly, if the salinity of reservoir brine is 200 000 ppm, the concentration of CO_2 should be around 20.05−50.65 mol % to obtain the same level of IFT at the NaCl concentration of 50 000 ppm at the pressure of 4351 psia and temperature of 257.0 °F, as shown in Figure 14.

4.4. IFT Modeling for $CO_2/CH_4/H_2O$ and CO_2/CH_4/Brine Systems. *4.4.1. Improved IFT Model for $CO_2/CH_4/H_2O$ Systems.* The IFT data for $CO_2/CH_4/H_2O$ systems are used to regress the coefficients appearing in eq 6. We obtain the following correlation based on regression analysis as indicated by Figure 15 (R^2 = 0.9658),

$$\sigma_{gw}^{0.25} = \frac{2.068}{T_r^{0.3125}}\left(\frac{M_H}{\sum_{i=1}^{n} z_i M_i}\right)^{0.183361} (\rho_M^L \sum_{i=1}^{n} x_i P_i - \rho_M^V \sum_{i=1}^{n} y_i P_i)^{0.2921} \quad (9)$$

Figure 16 presents a parity chart that plots the measured IFTs versus the calculated ones with eq 9, while Figure 17 shows the distribution of errors versus the number of data points. Both figures illustrate that a good match is obtained between the measured and calculated IFTs, demonstrating the accuracy of eq 9 in correlating the IFTs for $CO_2/CH_4/H_2O$ systems. Figure 17 indicates that the difference between

DOI: 10.1021/acs.iecr.6b02446
Ind. Eng. Chem. Res. 2016, 55, 12358−12375

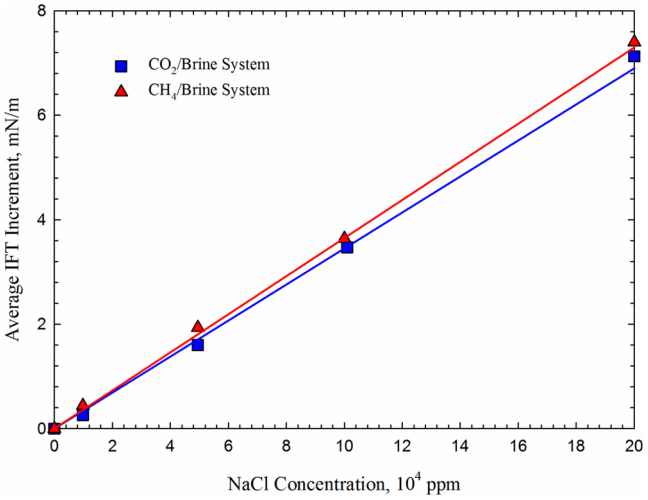

Figure 24. Average IFT increment for CO_2/brine and CH_4/brine systems as a function of NaCl concentration.

Table 4. Performance of the Improved IFT Model in Predicting the IFTs of $CO_2/CH_4/H_2O$ Systems Published by Ren et al.[11]

model	number of data points measured by Ren et al.[11]	AARE (%)	SD (%)
this study	150	10.19	14.01
Daneshet al.[4] 1998	150	57.92	62.82
Sutton[30] 2009	150	45.83	50.08
Firoozabadi and Ramey[28] 1988	150	26.56	30.40
Weinaug and Katz[24] 1943	150	26.45	32.67

predicted and measured data is mostly less than ±5.00 mN/m. Table 3 summarizes the statistical analysis results on using the improved correlation. As shown in Table 3, the average absolute relative error (AARE) and standard deviation (SD) are found to be 9.42% and 11.33%, respectively.

4.4.2. Comparison with Existing Correlations. The improved model is compared with four commonly used hydrocarbon gas/H_2O IFT correlations in the literature. As for the Firoozabadi and Ramey[28] correlation, a relationship between $\frac{\sigma_{gw}^{0.25}}{(\rho_L - \rho_V)} T_r^{0.3125}$ and $(\rho_L - \rho_V)$ can be obtained by plotting these two terms together, and then applying proper regression, as done in Figure 18. The following equation is obtained:

$$\sigma_{gw}^{0.25} = \frac{2.978}{T_r^{0.3125}} (\rho_L - \rho_V)^{0.1382} \quad (10)$$

Figure 19 shows a parity chart that compares the measured and calculated IFTs with eq 10. Similarly, three commonly used correlations (those of Sutton,[30] Danesh,[4] and Weinaug and Katz[24]) are also used to correlate the IFT data, as shown in Figures 20–22. Table 3 summarizes the overall comparison results, while Table S2 (shown in the Supporting Information) provides detailed comparison results between the measured IFTs and calculated IFTs with these correlations. As can be seen from Figures 19–22 and Table 3, there is a large discrepancy between the measured IFTs and calculated IFTs with these four models. Compared with these four correlations, eq 9 provides more accurate IFT prediction for the $CO_2/CH_4/H_2O$ systems.

4.4.3. Validation of the Improved Model. In order to further test the predictive ability of the newly developed IFT model, eq 9 is tested with 150 IFT data presented by Ren et al.[11] that are not used in developing the new IFT model. The comparison between the calculated and measured IFT values is presented in Figure 23. It indicates that the new IFT model provides a good prediction on $CO_2/CH_4/H_2O$ IFT. Deviations between the measured and predicted IFTs are mostly less than ±5.00 mN/m. Table 4 shows the validation results. Compared to other models, the improved model provides more accurate IFT prediction for $CO_2/CH_4/H_2O$ systems, with AARE and SD of 10.19% and 14.01%, respectively.

4.4.4. IFT Modeling for CO_2/CH_4/Brine Systems. The preceding discussion shows that salinity can increase the IFT of $CO_2/CH_4/H_2O$ systems. Some researchers[6,29] proposed to use a linear relationship to account for the IFT increase as a function of salinity. It can be seen from Figures 9 and 10 that, after the IFT levels off, the IFT increase due to salinity effect tends to be independent of temperature and pressure. As for the CO_2/brine (NaCl) systems, the following linear relationship is found to be adequate to account for the salinity effect, as shown in Figure 24:

$$\sigma_{cor-CO_2} = 3.45 \times 10^{-5} C_S \quad (11)$$

As for the CH_4/brine (NaCl) systems, the following linear relationship is obtained, as shown in Figure 24:

$$\sigma_{cor-CH_4} = 3.65 \times 10^{-5} C_S \quad (12)$$

The ratio of 3.600×10^{-5} obtained for CO_2/brine (NaCl) system is slightly different from the values reported in the literature. Chalbaud et al.[6] reported a ratio of 2.550×10^{-5} instead of 3.600×10^{-5} for the CO_2/brine system (up to 16 071 ppm of NaCl). Massoudi and King[12] reported a ratio of 2.704×10^{-5}, while Argaud[29] obtained a ratio of 2.789×10^{-5} for the CO_2/brine system. The ratio of 3.950×10^{-5} obtained in this study for CH_4/brine systems is larger than that of CO_2/brine systems. It indicates that an increase in salinity (NaCl) results in a more pronounced increase in the IFT for CH_4/brine systems than for CO_2/brine systems. Cai et al.[77] measured IFT of salt solutions containing NaCl, $CaCl_2$, and $MgCl_2$ with n-C_8H_{18}. They showed that the degree of IFT increase is sensitive to salt species. For salts such as KCl, $CaCl_2$ and $MgCl_2$, the effect of salt on IFT has been widely studied, and such increase in IFT is not linear at salt concentrations higher than 1.0 mol/kg. It is noted that one can first calculate the IFT of $CO_2/CH_4/H_2O$ system with eq 9 and then apply eqs 8, 11, and 12 to obtain the IFT of a given CO_2/CH_4/brine (NaCl) system.

5. CONCLUSIONS

Experiments were conducted to measure IFTs for the CO_2/CH_4/brine system along three isotherms between 77.0 and 257.0 °F, at pressures up to 5027 psia and salinities up to 200 000 ppm. Different CH_4/CO_2 ratios in the gas mixture were considered in the measurements. The IFT data measured for CO_2/H_2O and CH_4/H_2O mixtures were shown to be in good agreement with the published data, validating the reliability of our IFT measurements.

A detailed analysis of the CO_2 and salt effect on IFT was carried out based on the measured IFT data. The presence of

DOI: 10.1021/acs.iecr.6b02446
Ind. Eng. Chem. Res. 2016, 55, 12358–12375

CO_2 decreases the IFT, but the degree of reduction in IFT depends on the amount of CO_2 added. The presence of salt in pure water increases the IFT between gas and liquid. IFT reduction of the CH_4/brine system due to the addition of CO_2 can possibly result in an increased capillary number, which may be beneficial for enhancing shale gas recovery if CO_2 is used as a recovery medium.

Based on the IFT data measured in this research, an improved IFT correlation was developed based on the Parachor model[24] and Firoozabadi and Ramey's model.[28] Unlike other correlations, the improved IFT correlation accounts for all major parameters that affect $CO_2/CH_4/H_2O$ IFT, including pressure, temperature, individual compound's molecular weight, density difference, and gas composition on IFT of gas-mixture/H_2O systems. For the $CO_2/CH_4/H_2O$ mixtures, the improved correlation provides a more accurate prediction of $CO_2/CH_4/H_2O$ IFT data measured by Ren et al.[11] in comparison to other four existing correlations. Improved correlations used for predicting IFT of CO_2/CH_4/brine systems have been also presented, showing a good performance in correlating the measured IFTs.

■ ASSOCIATED CONTENT

Supporting Information

The Supporting Information is available free of charge on the ACS Publications website at DOI: 10.1021/acs.iecr.6b02446.

IFT data for CO_2/CH_4/brine systems at different temperatures and pressures, comparison of the measured IFTs for $CO_2/CH_4/H_2O$ systems with the IFTs calculated by eq 9 and four other existing correlations, and three parameters used for performing statistical error analysis (Appendix S1: Error Analysis) (PDF)

■ AUTHOR INFORMATION

Corresponding Author

*E-mail: huazhou@ualberta.ca. Phone: 1-780-492-1738 (H.A.L.).

ORCID

Huazhou Andy Li: 0000-0002-4541-670X

Ryosuke Okuno: 0000-0003-3675-1132

Notes

The authors declare no competing financial interest.

■ ACKNOWLEDGMENTS

The authors acknowledge a Discovery Grant from the Natural Sciences and Engineering Research Council (NSERC) of Canada to H.L. (NSERC RGPIN 05394) and China Scholarship Council (CSC) for financial support to Y.L. (201406450028). R.O. holds the Pioneer Corporation Faculty Fellowship in Petroleum Engineering at the University of Texas at Austin. The first author also thanks lab technicians Mr. Todd Kinnee, Mrs. Georgeta Istratescu, and Mr. Lixing Lin for their experimental support. Finally, the authors are grateful for Dr. Tayfun Babadagli's lab for accessing the IFT apparatus.

■ REFERENCES

(1) Heller, R.; Zoback, M. Adsorption of Methane and Carbon Dioxide on Gas Shale and Pure Mineral Samples. *J. Unconv. Oil Gas Resour.* **2014**, *8*, 14.

(2) Hussen, C.; Amin, R.; Madden, G.; Evans, B. Reservoir Simulation for Enhanced Gas Recovery: An Economic Evaluation. *J. Nat. Gas Sci. Eng.* **2012**, *5*, 42.

(3) Li, X.; Elsworth, D. Geomechanics of CO_2 Enhanced Shale Gas Recovery. *J. Nat. Gas Sci. Eng.* **2015**, *26*, 1607.

(4) Danesh, A. PVT and Phase Behaviour of Petroleum Reservoir Fluids. Ph.D. Dissertation, Herriot Watt University, Edinburgh, SCO, 1998.

(5) Li, Z.; Wang, S.; Li, S.; Liu, W.; Li, B.; Lv, Q. C. Accurate Determination of the CO_2-Brine Interfacial Tension Using Graphical Alternating Conditional Expectation. *Energy Fuels* **2014**, *28*, 624.

(6) Chalbaud, C.; Robin, M.; Egermann, P. Interfacial Tension Data and Correlations of Brine/CO_2 Systems under Reservoir Conditions. Presented at the SPE Annual Technical Conference and Exhibition, San Antonio, September 2006; SPE 102918.

(7) Aggelopoulos, C. A.; Robin, M.; Perfetti, M.; Vizika, O. CO_2/$CaCl_2$ Solution Interfacial Tensions under CO_2 Geological Storage Conditions: Influence of Cation Valence on Interfacial Tension. *Adv. Water Resour.* **2010**, *33*, 691.

(8) Shah, V.; Broseta, D.; Mouronval, G.; Montel, F. Water/acid Gas Interfacial Tensions and Their Impact on Acid Gas Geological Storage. *Int. J. Greenhouse Gas Control* **2008**, *2*, 594.

(9) Bahramian, A.; Danesh, A. Prediction of Liquid-Liquid Interfacial Tension in Multi-Component Systems. *Fluid Phase Equilib.* **2004**, *221*, 197.

(10) Bahramian, A.; Danesh, A. Prediction of Liquid-Vapour Surface Tension in Multi-Component Systems. *Fluid Phase Equilib.* **2005**, *236*, 156.

(11) Ren, Q. Y.; Chen, G. J.; Yan, W.; Guo, T. M. Interfacial Tension of (CO_2+CH_4)+Water from 298 to 373 K and Pressures up to 30 MPa. *J. Chem. Eng. Data* **2000**, *45*, 610.

(12) Massoudi, R.; King, A. D. Effect of Pressure on the Surface Tension of Aqueous Solutions. Adsorption of Hydrocarbon Gases, Carbon Dioxide, and Nitrous Oxide on Aqueous Solutions of Sodium Chloride and Tetra-n-Butylammonium Bromide at 25 °C. *J. Phys. Chem.* **1975**, *79*, 1670.

(13) Li, X.; Boek, E.; Maitland, G. C.; Trusler, J. P. M. Interfacial Tension of (Brines+CO_2): (0.864 NaCl+0.136 KCl) at Temperatures between (298 and 448) K, Pressures between (2 and 50) MPa, and Total Molarities of (1 to 5) mol·kg^{-1}. *J. Chem. Eng. Data* **2012**, *57*, 1078.

(14) Li, X.; Boek, E.; Maitland, G. C.; Trusler, J. P. M. Interfacial Tension of (Brines+CO_2): $CaCl_2$(aq), $MgCl_2$(aq), and Na_2SO_4(aq) at Temperatures between (343 and 423) K, Pressures between (2 and 50) MPa, and Molarities of (0.5 to 5) mol·kg^{-1}. *J. Chem. Eng. Data* **2012**, *57*, 1369.

(15) Kashefi, K.; Pereira, L. M. C.; Chapoy, A.; Burgass, R.; Tohidi, B. Measurement and Modelling of Interfacial Tension in Methane/Water and Methane/Brine Systems at Reservoir Conditions. *Fluid Phase Equilib.* **2016**, *409*, 301.

(16) Ralston, J.; Healy, T. Specific Cation Effects on Water Structure at the Air-Water and Air-Octadecanol Monolayer-Water Interface. *J. Colloid Interface Sci.* **1973**, *42*, 629.

(17) Johansson, K.; Eriksson, J. C. γ and dγ/dT Measurements on Aqueous Solutions of 1,1-Electrolyte. *J. Colloid Interface Sci.* **1974**, *49*, 469.

(18) Pegram, L. M.; Record, M. T. The Thermodynamic Origin of Hofmeister Ion Effects. *J. Phys. Chem. B* **2008**, *112*, 9428.

(19) Levin, Y.; dos Santos, A. P.; Diehl, A. Ions at the Air-Water Interface: An End to a Hundred-Year-Old Mystery? *Phys. Rev. Lett.* **2009**, *103*, 1.

(20) Yang, D. Y.; Tontiwachwuthikul, P.; Gu, Y. A. Interfacial Interactions between Reservoir Brine and CO_2 at High Pressures and Elevated Temperatures. *Energy Fuels* **2005**, *19*, 216.

(21) Bennion, D. B.; Bachu, S. A Correlation of the Interfacial Tension between Supercritical Phase CO_2 and Equilibrium Brine as a Function of Salinity, Temperature and Pressure. Presented at the SPE Annual Technical Conference and Exhibition, Colorado, September 2008; SPE 114479.

(22) Chalbaud, C.; Robin, M.; Lombard, J. M.; Bertin, H.; Egermann, P. Brine/CO_2 Interfacial Properties and Effects on CO_2 Storage in Deep Saline Aquifers. *Oil Gas Sci. Technol.* **2010**, *65*, 541.

DOI: 10.1021/acs.iecr.6b02446
Ind. Eng. Chem. Res. 2016, 55, 12358−12375

(23) Bachu, S.; Bennion, D. B. Interfacial Tension between CO_2, Freshwater, and Brine in the Range of Pressure from (2 to 27) MPa, Temperature from (20 to 125) °C, and Water Salinity from (0 to 334 000) mg·L^{-1}. *J. Chem. Eng. Data* **2009**, *54*, 765.
(24) Weinaug, C. F.; Katz, D. L. Surface Tension of Methane-Propane Mixtures. *Ind. Eng. Chem.* **1943**, *35*, 239.
(25) Macleod, D. B. On a Relation between Surface Tension and Density. *Trans. Faraday Soc.* **1923**, *19*, 38.
(26) Lee, S. T.; Chien, M. C. H. A New Multicomponent Surface Tension Correlation Based on Scaling Theory. Presented at the SPE/DOE Improved Oil Recovery Conference, Tulsa, April 1984; SPE/DOE 12643.
(27) Massoudi, R.; King, A. D., Jr. Effect of Pressure on the Surface Tension of Water Adsorption of Low Molecular Weight Gases on Water at 25 °C. *J. Phys. Chem.* **1974**, *78*, 2262.
(28) Firoozabadi, A.; Ramey, H. J., Jr. Surface Tension of Water-Hydrocarbon Systems at Reservoir Conditions. *J. Can. Pet. Technol.* **1988**, *27*, 41.
(29) Argaud, M. J. Predicting the Interfacial Tension of Brine/Gas (or Condensate) Systems. Presented at the SCA European Core Analysis Symposium, Paris, September, 1992.
(30) Sutton, R. P. An Improved Model for Water-Hydrocarbon Surface Tension at Reservoir Conditions. Presented at the SPE Annual Technical Conference and Exhibition, New Orleans, October 2009; SPE 124968.
(31) Hebach, A.; Oberhof, A.; Dahmen, N.; Kogel, A.; Ederer, H.; Dinjus, E. Interfacial Tension at Elevated Pressures-Measurements and Correlations in the Water+Carbon Dioxide System. *J. Chem. Eng. Data* **2002**, *47*, 1540.
(32) Kvamme, B.; Kuznetsova, T.; Hebach, A.; Oberhof, A.; Lunde, E. Measurements and Modelling of Interfacial Tension for Water +Carbon Dioxide Systems at Elevated Pressures. *Comput. Mater. Sci.* **2007**, *38*, 506.
(33) Chalbaud, C.; Robin, M.; Lombard, J. M.; Martin, F.; Egermann, P.; Bertin, H. Interfacial Tension Measurement and Wettability Evaluation for Geological CO_2 Storage. *Adv. Water Resour.* **2009**, *32*, 98.
(34) Yan, W.; Zhao, G.; Chen, G.; Guo, T. Interfacial Tension of (Methane+Nitrogen)+Water and (Carbon Dioxide+Nitrogen)+Water Systems. *J. Chem. Eng. Data* **2001**, *46*, 1544.
(35) Nordholm, S.; Johnson, M.; Freasier, B. C. Generalized van der Waals Theory. III. The Prediction of Hard Sphere Structure. *Aust. J. Chem.* **1980**, *33*, 2139.
(36) Cahn, J. W.; Hilliard, J. E. Free Energy of a Nonuniform System. I. Interfacial Free Energy. *J. Chem. Phys.* **1958**, *28*, 258.
(37) Rowlinson, J. S. Translation of J. D. van der Waals' "The Thermodynamic Theory of Capillarity under the Hypothesis of a Continuous Variation of Density. *J. Stat. Phys.* **1979**, *20*, 197.
(38) Evans, R. The Nature of the Liquid-Vapor Interface and Other Topics in the Statistical Mechanics of Non-Uniform, Classical Fluids. *Adv. Phys.* **1979**, *28*, 143.
(39) Almeida, B. S.; Telo da Gama, M. M. Surface Tension of Simple Mixtures: Comparison between Theory and Experiment. *J. Phys. Chem.* **1989**, *93*, 4132.
(40) Bongiorno, V.; Davis, H. T. Modified van der Waals Theory of Fluid Interfaces. *Phys. Rev. A: At., Mol., Opt. Phys.* **1975**, *12*, 2213.
(41) Li, X.; Yang, D. Determination of Mutual Solubility between CO_2 and Water by Using the Peng-Robinson Equation of State with Modified Alpha Function and binary Interaction Parameter. *Ind. Eng. Chem. Res.* **2013**, *52*, 13829.
(42) Søreide, I.; Whitson, C. H. Peng-Robinson prediction for hydrocarbons, CO_2, N_2, and H_2S with pure water and NaCl brine. *Fluid Phase Equilib.* **1992**, *77*, 217.
(43) Shariat, A. Measurement and Modelling of Interfacial Tension at High Pressure/High Temperature Conditions. Ph.D. Dissertation, University of Calgary, Calgary, AB, 2014.
(44) Zuo, Y. X.; Stenby, E. H. Corresponding-States and Parachor Models for the Calculation of Interfacial Tensions. *Can. J. Chem. Eng.* **1997**, *75*, 1130.
(45) Sato, K. Sensitivity of Interfacial-tension Predictions to Parachor-method Parameters. *J. Jpn. Pet. Inst.* **2003**, *46*, 148.
(46) Ayirala, S. C.; Rao, D. N. Application of a New Mechanistic Parachor Model to Predict Dynamic Gas-Oil Miscibility in Reservoir Crude Oil-Solvent Systems. Presented at the SPE International Petroleum Conference, Puebla, November 2004; SPE 91920.
(47) Fawcett, M. J. Evaluation of Correlations and Parachors to Predict Low Interfacial Tensions in Condensate Systems. Presented at the SPE 69th Annual Technical Conference and Exhibition, New Orleans, September 1994; SPE 28611.
(48) Hough, E. W.; Stegemeier, G. L. Correlation of Surface and Interfacial Tension of Light Hydrocarbons in the Critical Region. *SPEJ, Soc. Pet. Eng. J.* **1961**, *1*, 259.
(49) Ayirala, S. C.; Rao, D. N. A New Mechanistic Parachor Model to Predict Dynamic Interfacial Tension and Miscibility in Multicomponent Hydrocarbon Systems. *J. Colloid Interface Sci.* **2006**, *299*, 321.
(50) Sugden, S. Capillary Rise. *J. Chem. Soc., Trans.* **1921**, *119*, 1483.
(51) Quayle, O. R. The Parachors of Organic Compounds. An Interpretation and Catalogue. *Chem. Rev.* **1953**, *53*, 439.
(52) Standing, M. B. *Volumetric and Phase Behaviour of Oil Hydrocarbon Systems*; California Research Corp.: Dallas, 1951.
(53) Hough, E. W.; Rzasa, M. J.; Wood, B. B. Interfacial Tensions at Reservoir Pressures and Temperatures; Apparatus and the Water-Methane Systems. *JPT, J. Pet. Technol.* **1951**, *3*, 57.
(54) Jennings, H. Y.; Newman, G. H. The Effect of Temperature and Pressure on the Interfacial Tension of Water against Methane-Normal Decane Mixtures. *SPEJ, Soc. Pet. Eng. J.* **1971**, *11*, 171.
(55) Sachs, W.; Meyn, V. Pressure and Temperature Dependence of the Surface Tension in the System Natural Gas/Water: Principles of Investigation and the First Precise Experimental Data for Pure Methane/Water at 25 °C up to 48.8 MPa. *Colloids Surf., A* **1995**, *94*, 291.
(56) Khosharay, S.; Varaminian, F. Experimental and Modeling Investigation on Surface Tension and Surface Properties of (CH_4+H_2O), (C_2H_6+H_2O), (CO_2+H_2O) and (C_3H_8+H_2O) from 284.15 to 312.15 K and Pressures up to 60 bar. *Int. J. Refrig.* **2014**, *47*, 26.
(57) Hocott, C. R. Interfacial Tension between Water and Oil under Reservoir Conditions. *Trans. Soc. Pet. Eng.* **1939**, *132*, 184.
(58) Heuer, G. J. Interfacial Tension of Water against Hydrocarbons and Other Gases and Adsorption of Methane on Solids at Reservoir Temperatures and Pressures. Ph.D. Dissertation, University of Texas, Austin, TX, 1957.
(59) Chun, B. S.; Wilkinson, G. T. Interfacial Tension in High-Pressure Carbon Dioxide Mixtures. *Ind. Eng. Chem. Res.* **1995**, *34*, 4371.
(60) da Rocha, S. R. P.; Harrison, K. L.; Johnston, K. P. Effect of Surfactants on the Interfacial Tension and Emulsion Formation between Water and Carbon Dioxide. *Langmuir* **1999**, *15*, 419.
(61) Park, J. Y.; Lim, J. S.; Yoon, C. H.; Lee, C. H.; Park, K. P. Effect of a Fluorinated Sodium Bis (2-Ethylhexyl) Sulfosuccinate (Aerosol-OT, AOT) Analogue Surfactant on the Interfacial Tension of CO_2+Water and CO_2+Ni-Plating Solution in Near- and Supercritical CO_2. *J. Chem. Eng. Data* **2005**, *50*, 299.
(62) Chiquet, P.; Daridon, J.; Broseta, D.; Thibeau, S. CO_2/Water Interfacial Tensions under Pressure and Temperature Conditions of CO_2 Geological Storage. *Energy Convers. Manage.* **2007**, *48*, 736.
(63) Georgiadis, A.; Maitland, G.; Trusler, J. P. M.; Bismarck, A. Interfacial Tension Measurements of the (H_2O+CO_2) System at Elevated Pressures and Temperatures. *J. Chem. Eng. Data* **2010**, *55*, 4168.
(64) Petrova, T. Revised Release on Surface Tension of Ordinary Water Substance. Presented at the International Association for the Properties of Water and Steam, Moscow, 2014.
(65) Duan, Z.; Sun, R. An Improved Model Calculating CO_2 Solubility in Pure Water and Aqueous NaCl Solutions from 273 to 533 K and from 0 to 2000 bar. *Chem. Geol.* **2003**, *193*, 257.

DOI: 10.1021/acs.iecr.6b02446
Ind. Eng. Chem. Res. 2016, 55, 12358−12375

(66) Bando, S.; Takemura, F.; Nishio, M.; Hihara, E.; Akai, M. Solubility of CO_2 in Aqueous Solutions of NaCl at (30 to 60) °C and (10 to 20) MPa. *J. Chem. Eng. Data* **2003**, *48*, 576.
(67) Koschel, D.; Coxam, J. Y.; Majer, V.; et al. Enthalpy and Solubility Data of CO_2 in Water and NaCl (aq) at Conditions of Interest for Geological Sequestration. *Fluid Phase Equilib.* **2006**, *247*, 107.
(68) Whitson, C. H.; Brulé, M. R. *Phase Behavior*; Henry L. Doherty Memorial Fund of AIME Society of Petroleum Engineers Inc.: Richardson, TX, 2000.
(69) Wiebe, R. The Brine System Carbon Dioxide-Water under Pressure. *Chem. Rev.* **1941**, *29*, 475.
(70) Malinin, S. D.; Kurovskaya, N. A. Solubility of CO_2 in Chloride Solutions at Elevated Temperatures and CO_2 Pressures. *Geochem. Int.* **1975**, *2*, 199.
(71) Malinin, S. D.; Savelyeva, N. I. The Solubility of CO_2 in NaCl and $CaCl_2$ Solutions at 25, 50 and 75 °C under Elevated CO_2 Pressures. *Geochem. Int.* **1972**, *9*, 410.
(72) Wiegand, G.; Franck, E. U. Interfacial Tension between Water and Non-polar Fluids up to 473 K and 2800 bar. *Ber. Bunsenges. Phys. Chem.* **1994**, *98*, 809.
(73) Abramzon, A. A.; Gaukhberg, R. D. Surface Tension of Salt Solutions. *Russian J. Appl. Chem.* **1993**, *66*, 1428.
(74) Chen, Z.; Xia, S.; Ma, P. Measuring Surface Tension of Liquids at High Temperature and Elevated Pressure. *J. Chem. Eng. Data* **2008**, *53*, 742.
(75) Firoozabadi, A. *Thermodynamics and Applications in Hydrocarbon Energy Production*; McGraw Hill Education: New York, 2016.
(76) Rushing, J. A.; Newsham, K. E.; Van Fraassen, K. C.; Mehta, S. A.; Moore, G. R. Laboratory Measurements of Gas-Water Interfacial Tension at HP/HT Reservoir Conditions. Presented at the CIPC/SPE Gas Technology Symposium, Calgary, June 2008; SPE 114516.
(77) Cai, B. Y.; Yang, J. T.; Guo, T. M. Interfacial Tension of Hydrocarbon+Water/Brines Systems under High Pressure. *J. Chem. Eng. Data* **1996**, *41*, 493.
(78) Jho, C.; Nealon, D.; Shogbola, S.; King, A. D. Effect of Pressure on the Surface Tension of Water: Adsorption of Hydrocarbon Gases and Carbon Dioxide on Water at Temperatures between 0 and 50°C. *J. Colloid Interface Sci.* **1978**, *65*, 141.
(79) Lepski, B. Gravity Assisted Tertiary Gas Injection Process In Water Drive Oil Reservoirs. Ph.D. Dissertation, Louisiana State University, Baton Rouge, USA, 1997.
(80) Tian, Y.; Xiao, Y.; Zhu, H.; Dong, X.; Ren, X.; Zhang, F. Interfacial Tension between Water and Non-Polar Fluids at High Pressures and High Temperatures. *Acta Physico-Chimica Sinica.* **1997**, *13*, 89.
(81) Zhao, G. Y. Measurement and Calculation of High Pressure Interfacial Tension of Methane Nitrogen/Water System. *J. Univ. Pet.* **2002**, *26*, 75.
(82) Tewes, F.; Boury, F. Formation and Rheological Properties of the Supercritical CO_2-Water Pure Interface. *J. Phys. Chem. B* **2005**, *109*, 3990.
(83) Akutsu, T.; et al. Interfacial Tension between Water and High Pressure CO_2 in the Presence of Hydrocarbon Surfactants. *Fluid Phase Equilib.* **2007**, *257*, 163.
(84) Sutjiadi-Sia, Y.; Jaeger, P.; Eggers, R. Interfacial Phenomena of Aqueous Systems in Dense Carbon Dioxide. *J. Supercrit. Fluids* **2008**, *46*, 272.
(85) Shariat, A.; Moore, R. G.; Mehta, S. A.; Van Fraassen, K. C.; Newsham, K. E.; Rushing, J. A. A Laboratory Study of the Effects of Fluid Compositions on Gas-Water Interfacial Tension at HP/HT Reservoir Conditions. Presented at the SPE Annual Technical Conference and Exhibition, Denver, October 30−November 2, 2011; SPE 146178.
(86) Aggelopoulos, C. A.; Robin, M.; Vizika, O. Interfacial Tension between CO_2 and Brine ($NaCl+CaCl_2$) at Elevated Pressures and Temperatures: The Additive Effect of Different Salts. *Adv. Water Resour.* **2011**, *34*, 505.
(87) Shariat, A.; Moore, R. G.; Mehta, S. A.; Fraassen, K.; Newsham, K.; Rushing, J. A. Laboratory Measurement of CO_2−H_2O Interfacial Tension at HP/HT Conditions: Implications for CO_2 Sequestration in Deep Aquifers. Presented at the Carbon Management Technology Conference, Orlando, February 2012; Paper 150010.
(88) Pereira, L. M. C.; Chapoy, A.; Burgass, R.; Oliveira, M. B.; Coutinho, J. A. P.; Tohidi, B. Study of the Impact of High Temperature and Pressures on the Equilibrium Densities and Interfacial Tension of the Carbon Dioxide/Water System. *J. Chem. Thermodyn.* **2016**, *93*, 404.

DOI: 10.1021/acs.iecr.6b02446
Ind. Eng. Chem. Res. 2016, 55, 12358−12375